Soils and Foundations 2013;53(3):443–461

The Japanese Geotechnical Society

Soils and Foundations

www.sciencedirect.com
journal homepage: www.elsevier.com/locate/sandf

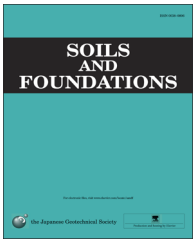

Rainfall-induced failures of volcanic slopes subjected to freezing and thawing

Shima Kawamura[a,*], Seiichi Miura[b]

[a]Graduate School of Engineering, Muroran Institute of Technology, 27-1 Mizumoto-cho, Muroran 050-8585, Japan
[b]Graduate School of Engineering, Hokkaido University, Kita 13 Nishi 8, Kita-ku, Sapporo 060-8264, Japan

Received 24 July 2012; received in revised form 29 January 2013; accepted 23 February 2013
Available online 20 May 2013

Abstract

Rainfall- and earthquake-induced failures of slopes formed by volcanic soils occur frequently in Hokkaido, Japan. The aim of this study is to clarify the failure mechanisms of volcanic slopes caused by both rainfall and freeze–thaw action in cold regions such as Hokkaido. Using model slopes of different shapes formed by volcanic soils, a series of rainfall tests are conducted under field conditions in which a spray nozzle is used to simulate rainfall intensity. Test results show that the surface failure of volcanic slopes differs depending strongly on the angle and the initial moisture content of the slopes. Based on the results of the model testing, the effects of freezing and thawing on the failure mechanism are drawn upon to propose an evaluation method for slope stability. In consideration of the model test results, it is found that the formation of a frozen layer and the softening of the slope surface, due to the freeze–thaw action, are significant for the stability of volcanic slopes in cold regions, and that slope failure can be uniquely assessed by the changes in water content in zones subjected to rainfall and freeze–thaw action.

Keywords: Freeze–thaw action; Model test; Rainfall; Slope failure; Volcanic soils; IGC: E6/E14

1. Introduction

In cold regions, such as Hokkaido, Japan, the surface layer of the ground on slopes freezes during the winter months, and this frozen layer thaws from the surface during the spring months. It has been established that the failure pattern of slopes in cold regions is different from that in warm regions; however, the mechanism of slope failure has not yet been clarified. Therefore, it is necessary to reveal the effect of freeze–thaw action on failure mechanisms in order to evaluate slope stability in cold regions.

In Hokkaido, there are over 40 Quaternary volcanoes, and pyroclastic materials cover over 40% of these areas. Significant volcanic activity occurred in the Neogene's Quaternary period, and various pyroclastic materials, such as volcanic ash, pumice and scoria, formed during those eruptions. These volcanic soils have been utilized as useful construction material, especially in foundations or man-made earth structures (embankments and cut slopes, etc.). Since the 1980s, volcanic soils have been classified as "problematic soils" (IS-Tohoku98, 1998) and research on them, from an engineering standpoint, has been limited in comparison to cohesive and non-cohesive soils (e.g., Miura et al., 2003).

Recent earthquakes and heavy rainfall in Hokkaido have generated the most serious damage in the ground, in natural slopes, in cut slopes and in embankments which are composed of volcanic soils (e.g., JSSMFE, 1995; JSCE, 2004). Examples include the slope failure of a residential embankment, due to

*Corresponding author.
E-mail addresses: skawamur@mmm.muroran-it.ac.jp (S. Kawamura), s-miura@eng.hokudai.ac.jp (S. Miura).

Peer review under responsibility of The Japanese Geotechnical Society.

Production and hosting by Elsevier

0038-0806
http://dx.doi.org/10.1016/j.sandf.2013.04.006

the 1991 Kushiro-oki earthquake, and the failure of cut slopes along the Hokkaido Expressway, due to snowmelt (water produced by the thawing of snow) in the spring of 1999 (Yamazaki et al., 2000).

Fig. 1 shows the mechanism of frost-heaving in a cut slope and failure modes in cold regions. Slopes freeze from the surface with the formation of ice lenses during the winter season (see Fig. 1(a)). Thereafter, the frozen soil thaws gradually from the ground surface until the summer season. In the freezing and thawing sequence, the surface layer of a slope may exhibit a high moisture content over the liquid limit of its soil owing to the melting of snow and the thawing of the ice lenses. As a result, surface failure occurs at the boundary between the loose thawing soil and the frozen layer due to water infiltration from both rainfall and snowmelt, because the frozen layer works as an impermeable layer (see Fig. 1(b): failure pattern 1). On the other hand, another failure due to the piping phenomenon of groundwater may also be observed in the spring season when pore water pressure increases over the strength of the frozen layer (see Fig. 1(c): failure pattern 2). The reason for this is that the groundwater level increases with the formation of a frozen layer (Hokkaido Branch of JGS, 2010), as demonstrated in a latter discussion. In addition, the hollows of ice lenses created by thawing may generate looser structures in the frozen layer compared with before the freeze–thaw process (see Fig. 1(d): failure pattern 3). Due to this phenomenon, a deeper slope failure may be induced from summer to autumn seasons.

For the above reasons, natural disasters, such as slope failure, are frequently induced in cold regions in the snow-melting season and are deemed to be caused by both the increase in the degree of saturation arising from the thawing water and changes in the deformation–strength characteristics of the soil resulting from freeze–thaw action.

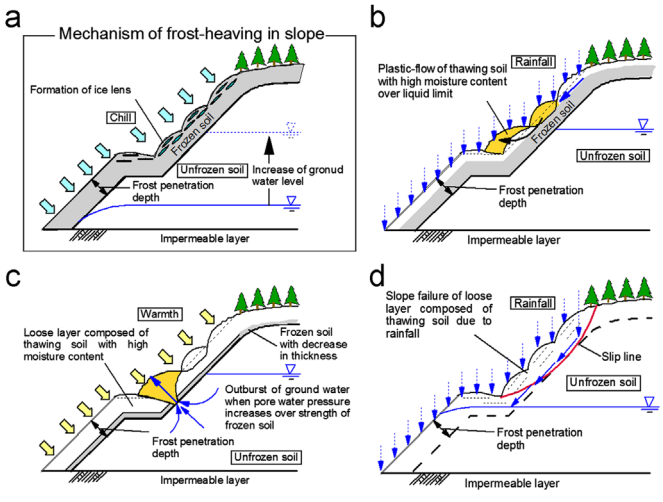

Fig. 1. Mechanism of frost-heaving in cut slope observed for cold regions and failure modes: (a) mechanism of frost-heaving in slope, (b) surface failure of thawing soil with high moisture content over liquid limit (failure pattern 1), (c) slope failure due to piping by increase in pore water pressure (failure pattern 2), and (d) slope failure of loose layer composed of thawing soil due to rainfall (failure pattern 3).

A significant amount of research has been conducted on the mechanisms of slope failure induced by rainfall in warm regions. Recently, research on slope failure mechanisms based on unsaturated mechanical behavior, as well as mechanisms caused by a decrease in effective stress under saturation, have been reported (e.g., Yatabe et al., 1986; Yagi et al., 1990; Orense, et al., 2004; Kitamura et al., 2007; Olivares et al., 2009; Kitamura and Sako, 2010; Jeng and Lin, 2011; Zhang et al., 2011). In particular, Yagi et al. (1990) have indicated the importance of the amount of limited rainfall and have proposed a prediction method for rainfall-induced failure based on field data and experimental data for Shirasu slopes. Additionally, predictions of slope failure through monitoring techniques, for instance, predictions using satellite systems, have been proposed (Kojima et al., 2003). Okimura (2006) and Kitamura and Sako (2010) have also created state-of-the-art methods for warm region slope failures. In particular, Kitamura and Sako (2010) have reviewed studies on rainfall-induced slope failures during the last 50 years and have indicated the importance of unsaturated soil mechanics in elucidating failure mechanisms. Torii et al. (2007) has also performed experimental studies on the failure mechanism of complex disasters with earthquakes and rainfall. Furthermore, a geo-and hydro-mechanical evaluation method for slope failure, based on the geotechnical investigation of geodisaster sites, has been conducted by Kasama et al. (2011).

Geotechnical problems due to frost-heaving and thawing action have been similarly reported in a number of studies (e.g., Aoyama et al., 1985; Nishimura et al., 1993; Ishikawa et al., 2008; Hokkaido Branch of JGS, 2010). The mechanical behavior of frozen and thawed soils has been clarified through these studies, and the importance of estimations to geotechnical problems has been elucidated.

Additionally, Harris and Davies (2000) and Harris and Lewkowicz (2000) have investigated the deformation behavior of slopes subjected to freezing and thawing for slope stability. However, in situ experimental and analytical studies on slope stability due to the freezing and thawing sequence have been rather limited.

The authors have similarly investigated rainfall-induced failures of volcanic slopes and their mechanisms (Kawamura et al., 2007, 2010a). In previous studies, a series of model tests was performed on volcanic and sandy slopes under several conditions. Rainfall intensities were 60 mm/h, 80 mm/h and 100 mm/h, which were accurately simulated through the use of spray nozzles. During the rainfall tests, deformation, pore water pressure behavior and the variation in saturation degree were monitored. The effects of the geometric condition of the slopes and of the rainfall conditions on the failure mechanisms were clarified in detail. As a result, it was demonstrated that the slope failures of volcanic soils depend strongly on both the angle of the slope and the friction of its impermeable layer; however, slope density was not shown to be a significant factor. It was also demonstrated that the cause of failure is not only the rise in water level from the base of the impermeable layer, but also the difference in the development of saturation (the difference in water retention characteristics of the volcanic slope, e.g., the changes in water content).

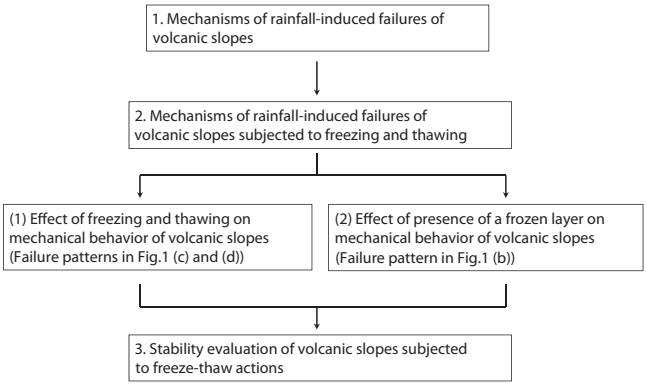

Fig. 2. Test scheme and flow of discussions.

The purposes of this paper are to reveal the failure mechanisms of volcanic slopes and to elucidate the effects of freezing and thawing phenomena on the mechanical behavior of volcanic slopes during rainfall. Fig. 2 illustrates the test scheme in this study. As shown in the figure, firstly, the surface failure mechanism of volcanic slopes due to rainfall is investigated to reveal the effects of the differences in slope angle, soil density and initial water content on the mechanical behavior and slope failure. Secondly, a series of model tests is conducted on volcanic slopes subjected to freeze–thaw action. In particular, the effect of freezing and thawing on the mechanical behavior and slope failure (see failure patterns shown in Fig. 1(c) and (d)) and the effect of the presence of a frozen layer on slope failure (see failure pattern shown in Fig. 1 (b)) are elucidated. Finally, an evaluation method considering the effects of freezing and thawing on slope stability is proposed based on the changes in water content in the slopes.

Test materials and test procedures

Test materials

Volcanic coarse-grained soils, sampled from the ejectas of Shikotsu and Mashu calderas in Hokkaido, were used in this study. The sampling sites are shown in Fig. 3. These samples are hereafter referred to as Kashiwabara (Spfa-1), Komaoka (Spfl) and Touhoro (Ma-l) volcanic soils. The index properties and the grain-size distribution curves of the samples are shown in Table 1 and Fig. 4, respectively, and are compared to the characteristics of Toyoura sand. As shown in Table 1 and Fig. 4, their fines contents range from 1.3% to 26%. In particular, the low value of dry density for Kashiwabara and Touhoro volcanic soils is also shown in the samples because their constituent particles are very porous and extremely vulnerable to crushing. On the other hand, the index properties of Komaoka volcanic soil differ from those of Kashiwabara volcanic soil due to the difference in deposits (flow-deposits: Spfl and fall-deposits: Spfa-1), although they are in the same Shikotsu ejecta. Details of the mechanical behavior of these volcanic soils have been described by Miura et al. (1996, 2003) and the Hokkaido Branch Research Committee, JGS (2011).

Fig. 3. Locations of sampling sites.

Table 1
Index properties of samples.

Sample name	ρ_s (g/cm^3)	$\rho_{d\ in\ situ}$ (g/cm^3)	$\rho_{d\ max}$ (g/cm^3)	$\rho_{d\ min}$ (g/cm^3)	w_n (%)	D_{50} (mm)	Uc	Fc (%)
Kashiwabara	2.34	0.53	0.55	0.35	60–80	1.3	3.1	1.3
Touhoro	2.59	0.44	0.85	0.52	106–206	7.60	7.0	1.3
Komaoka	2.50	–	1.12	0.76	34	0.27	3.6	26.0
Toyoura sand	2.68	–	1.63	1.37	–	0.18	1.5	0

w_n, natural water content; D_{50}, mean grain size; Uc, coefficient of uniformity; Fc, fines content.

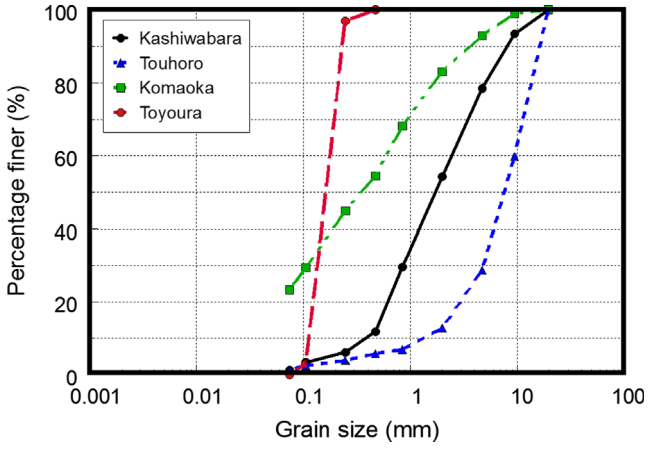

Fig. 4. Grain size distributions of samples.

Test procedures

It is impossible to accurately reproduce the mechanical behavior of a slope due to errors (the scale effect, the soil particle effect and the confining pressure effect, etc.) in the similitude scale, especially in the 1 g field. However, it is a genuine fact that a physical modeling in the model testing can increase our understanding.

In this model testing, it has been assumed that the strength of the soil varies proportionally to the normalization of the effective confining pressure in the slope. Namely the conventional way of thinking for element testing is taken in that of the 1 g model testing (see Fig. 5). Based on this technique, the mechanical behavior in the element of a slope for the 1 g model corresponds with that for the real field, if the rainfall intensity and the seepage speed in the model are consistent with those in the prototype. Owing to this, the rainfall intensity which was thought to exist in the real field was directly given to the slope surface, and volcanic coarse-grained soils were adopted as the test materials. As a result, the similarity of the dependency on time, regarding the development of pore water pressure and the consolidation phenomenon, may not be required theoretically. Additionally, it should be noted that the pore water pressure value obtained from the model testing can be similarly evaluated as a true value. Consequently, the reproduction by model testing is theoretically enabled, although the assumption that a model and a natural physical phenomenon occur in the same mechanism is required (Kawamura et al., 2010b). The correlation between the model and the prototype in this study is summarized in Table 2.

Table 3 illustrates the test conditions in this study. The following contents were concretely investigated:

(1) The clarification of the difference in behavior on the initial water content and the slope angle for each volcanic soil (cases 1–3, cases 6–8, cases 11 and 12).
(2) The presentation of the effect of freeze–thaw action on the mechanical behavior in the slope for each volcanic soil (cases 4 and 5, cases 9 and 10, cases 15–17).
(3) The elucidation of the effect of the presence of a frozen layer on the failure mechanism (cases 13–15).

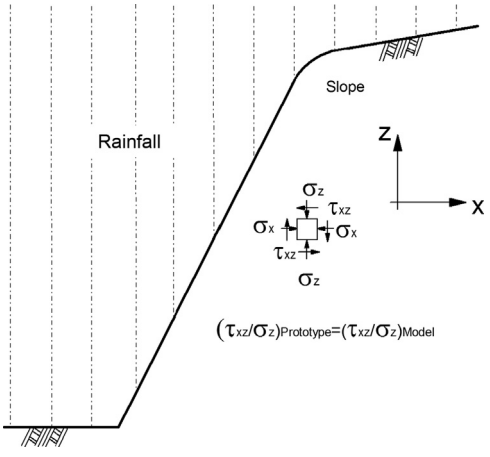

Fig. 5. Test concept for 1 g model test.

Table 2
Correlation between model and prototype.

Scale	Prototype/Model
Length	λ
Stress ratio in element in slope	1
Pore water pressure ratio	1
Strain in element of slope	1
Deformation	λ

Fig. 6 depicts a whole view of the apparatus used in the rainfall testing. The soil container was 2000 mm in length, 700 mm in depth and 600 mm in width, and its front wall was made of reinforced glass in order to observe deformation with failure. The model slopes were constructed by compacting or by air-pluviating so as to be the desired value (see Table 3, variations in dry density are within 5%, respectively) where constituent particles were not broken by compaction under the initial water contents. The desired initial water content of the model slope, w_0, is shown in Table 3. The weights of the rollers used for compaction and the number of compactions are summarized in Table 4. In general, it is supposed that the compacted density varies with the change in water content if the same compaction energy is adopted. However, the change in density was not recognized in this study. The reason is that the range between maximum and minimum densities is small for Kashiwabara and Touhoro volcanic soils.

For all the model tests, the difference in failure mechanism due to the 5% variation in the initial degree of saturation for each position was not observed (Kawamura et al., 2010a). As a result, the variation in initial saturation was set within 5%. Thereafter, the slope surface was carefully cut to angles of 45, 55, 60 and 65° (relative to horizontal) using a straight edge to eliminate surface disturbance. In order to appropriately simulate freezing and thawing action, the surface of the slope was frozen with dry ice over eight hours and was then thawed at 20 °C (over a basic thawing period of 8 h) after the model slope had been constructed. This is why the frost-heaving phenomenon was not sufficiently reproduced. The freezing–thawing phenomenon of the slope surface was intended in this study. According to this procedure, frozen layers are, 25–80 mm in thickness, formed for the Touhoro, Komaoka and Kashiwabara model slopes.

A rainfall intensity of 100 mm/h was typically adopted and was accurately simulated using a spray nozzle. In the case of an increase in groundwater, the water was supplied from the back of the model slopes and its water level was regulated using a sheet (a plastic plate) with an opening occupying 0.42% of the whole cross section area so as not to induce the piping phenomenon at the toe of the slope at the initial state. In this study, a hydraulic gradient of 1 was adopted because the water level of the water supply chamber became stable when the hydraulic gradient was 1. Thereafter, model tests were conducted immediately. Fig. 7 shows typical slope shapes (60- and 65-degree slopes) and the setting positions of the measurement devices. For 45- and 55-degree slopes, the measurement devices were basically set at the same positions as those for the 60- and 65-degree slopes (the depth from the slope surface and the elevation). For example, according to this model testing, the depths of the measurement devices in the real field can be converted by multiplying those in the model by λ times, as shown in Table 2.

The rainfall from the slope bottom was mandatorily drained by a pump. Therefore, the mechanical behavior of the slopes subjected to seepage water and the increase in underground

water from the back of the slopes due to rainfall were discussed.

During the rainfall testing, changes in deformation behavior, saturation degree and temperature were monitored using digital video cameras, soil moisture meters and thermocouple sensors, respectively. In particular, the deformation behavior was estimated according to a particle image velocimetry (PIV) analysis (White et al., 2003). Soil moisture meters were calibrated for several density conditions of the slopes. However, variations in soil moisture, attributed to the dilatancy induced by the deformation of the slopes during model testing, were not evaluated in the subsequent discussion due to the difficulty in defining its behavior.

Pore water pressure was monitored simultaneously. In a series of model tests, the negative pore water pressure due to suction exhibited small values. Owing to this, the influence of the dissipation of suction on slope instability was ignored (Kawamura et al., 2010a). This fact has also been confirmed by triaxial compression tests performed to reveal the effect of the decrease in suction on the shear strength of volcanic soils

Table 3
Test conditions for this study.

Notation of test case	Case 1	Case 2	Case 3	Case 4	Case 5	Case 6	Case 7	Case 8	Case 9	Case 10
Sample name	T-soil	T-soil	T-soil	T-soil	T-soil	Ko-soil	Ko-soil	Ko-soil	Ko-soil	Ko-soil
Slope condition	NFT	NFT	NFT	FT	FT	NFT	NFT	NFT	FT	FT
Slope angle (°)	55	60	65	55	65	45	55	65	45	65
Length of base, B (mm)	572	507	442	572	442	750	557	442	750	442
Initial water content (%)	45, 65, 80	65	45, 50, 65	45, 65, 80	45, 65, 80,100	34	34	34	34	34
Dry density ρ_d (g/cm^3)	0.44	0.44	0.44	0.44	0.44	0.9	0.9	0.9	0.9	0.9
Ranfall intensity, R (mm)	100	100	100	100	100	100	100	100	100	100
Freeze-thaw action cycles	–	–	–	1, 2	1	–	–	–	1, 2	1
Thaw time (h)	–	–	–	8	8	–	–	–	8	8
Other condition	–	–	–	–	–	–	–	–	–	–

Notation of test case	Case 11	Case 12	Case 13	Case 14	Case15	Case16	Case 17
Sample name	Ka-soil	Ka-soil	Ka-soil	Ka-soil	Ka-soil	Ka-soil	Ka-soil
Slope condition	NFT	NFT	NFT	F	FT	FT	FT
Slope angle (°)	60	65	60	65	60	60	65
Length of base, B (mm)	507	442	507	552	507	507	442
Initial water content (%)	70	20, 40, 55, 60, 70	70	70	70	70	20, 40, 55, 60, 70
Dry density ρ_d (g/cm^3)	0.45, 0.48	0.45, 0.48	0.45, 0.48	0.45, 0.48	0.45, 0.48	0.45, 0.48	0.45, 0.48
Ranfall intensity, R (mm)	100	100	–	100	–	100	100
Freeze-thaw action cycles	–	–	–	1	1	1	1, 2
Thaw time (h)	–	–	–	–	1	8	8
Other condition	–	–	Change in ground water level	Thickness of layer, 100mm	Change in ground water level	–	–

T-soil: Touhoro volcanic soil, Ko-soil: Komaoka volcanic soil, Ka-soil: Kashiwabara volcanic soil,
NFT: No freeze-thaw action, FT: Freeze-thaw action, F: Freeze action

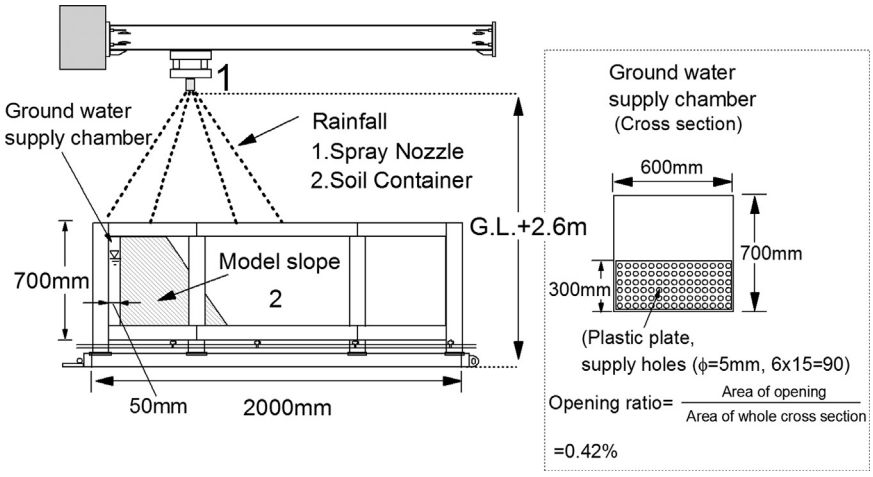

Fig. 6. Whole view of apparatus.

(Ishikawa et al., 2010). Furthermore, the pore water pressure behavior preceding failure was not sensitive compared to the behavior of soil moisture, as described in a latter discussion. Therefore, the emphasis of this study is on saturation. In subsequent discussions, the pore water pressure, normalized by the overburden pressure, was used as a parameter, because the conventional way of thinking regarding element testing is taken in that of the 1g model testing.

In previous studies, a series of model tests on Kashiwabara volcanic slopes was carried out in order to understand the effects of the changes in slope angle, soil density and friction of the impermeable layer in the slope on failures. In the present study, a series of rainfall tests with freeze–thaw action was conducted on a model slope simulating three types of failure patterns, as shown in Fig. 1. The rainfall model testing was performed for 3 h or until the slope failure was induced.

In order to define slope failure, the relative relations on the behavior until slope failure between saturation degree, pore water pressure and deformation were demonstrated on the basis of preliminary test data on Toyoura sand and Kashiwabara volcanic slopes (Kawamura et al., 2007, 2010a). Firstly, Fig. 8(a) and (b) illustrates the changes in pore water pressure and in saturation degree with elapsed time for the Toyoura sand slope. The Toyoura sand slope was constituted by pluviating Toyoura sand into air under dry conditions. The values at which large deformation was caused are depicted by a circle symbol. In Fig. 8, the pore water pressure and the degree of saturation rapidly develop with the increase in rainfall, thereafter becoming steady states. The soil moisture behavior is sensitive compared to the pore water pressure behavior, as shown in Fig. 8(b). Fig. 9(a) and (b) shows shear strain distributions at the peak of pore water pressure and the degree of saturation obtained from the PIV analysis, respec-

Table 4
Weight of roller and number of compactions for each case.

Sample name	Desired dry density (g/cm^3)	Initial water content (%)	Weight of roller (N)	Number of compactions (per layer)	Thickness of compaction layer (mm)
Touhoro	0.44	45, 50, 65, 80, 100	29.4	20	100
Komaoka	0.90	34	127.4	4	50
Kashiwabara	0.48	20, 40, 55, 60, 70	29.4	1	100
	0.45	20, 40, 55, 60, 70	–	0 (air pluviation)	–

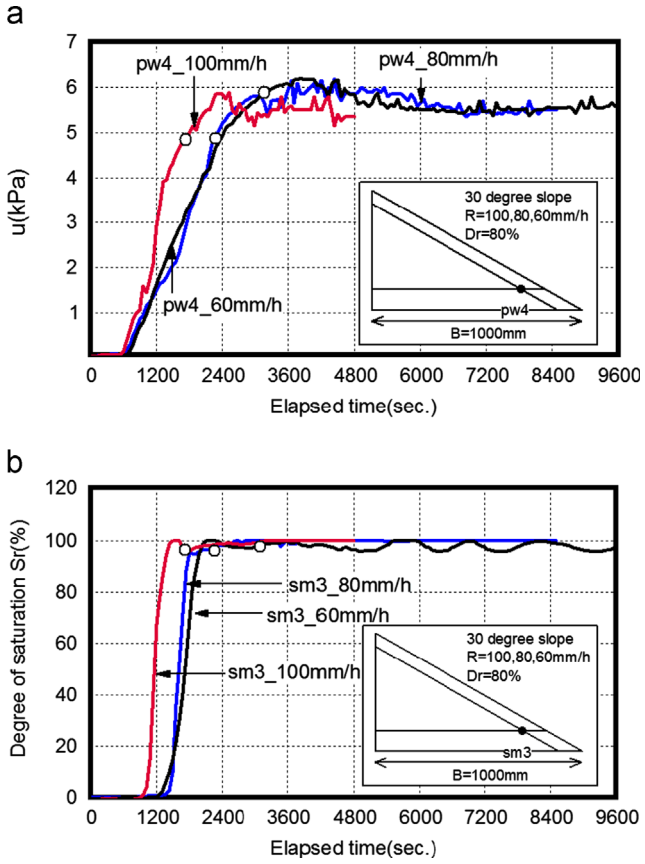

Fig. 8. Changes in pore water pressure and saturation degree with elapsed time for Toyoura sand slope: (a) pore water pressure and (b) saturation degree.

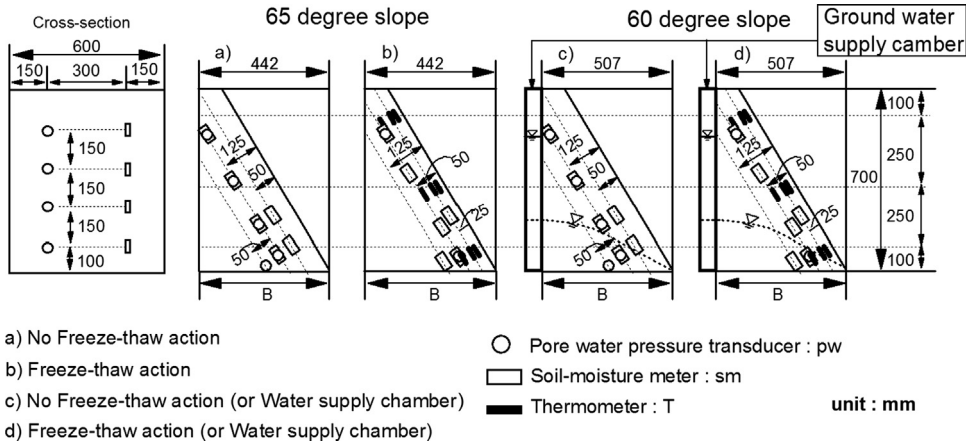

Fig. 7. Typical model shapes (60- and 65-degree slopes) and setting positions of measurement devices.

tively. As shown in these figures, the shear strain around the position of the pore water pressure transducer is 30%, whereas that around the soil moisture meter is 4–6%. Slope failure with large deformation developed rapidly after a shear strain of 4–6%. Therefore, it can be said that the degree of saturation is sensitive compared to that of pore water pressure in evaluating the behavior up to slope failure. A similar tendency was obtained for three other kinds of volcanic soil.

Secondly, Figs. 10 and 11 illustrate typical test results for the difference in rainfall intensity for Kashiwabara volcanic slopes reported in previous studies (e.g., Kawamura et al., 2010a) to examine the validity of the above results. The initial degrees of saturation for 100 mm/h and 60 mm/h were in the ranges of 43.9–49.3% and 42.9–47.2%, respectively. Variations in negative pore water pressure due to suction were of little significance, because the voids in this material were large. In the figures, μ means the friction coefficient of the surface of an impermeable layer. Details of the measurement procedures were also described by Kawamura et al. (2010a). It is apparent from the figures that the degree of saturation indicates the peak value at 245 s ($R=100$ mm/h) or 375 s ($R=60$ mm/h), thereafter slightly decreasing with the increase in deformation (see Fig. 10). However, apparent changes due to the development of a slip line were not recognized for the pore water pressure (see Fig. 11). In the shear strain at the peak degree of saturation, the strain was generally less than 4–6%, except for some areas of 8–30% (see Fig. 12(a) and (b)). Slope failure with large deformation developed rapidly after a shear strain of 4–6%, similar to the Toyoura sand slope. A similar tendency was obtained for other test cases irrespective of the differences in initial water content, slope angle and soil materials, although these cases are not depicted here.

For these reasons, the mechanical behavior at a shear strain of 4–6% by the PIV analysis was regarded as that of the plastic equilibrium state, namely, that at failure.

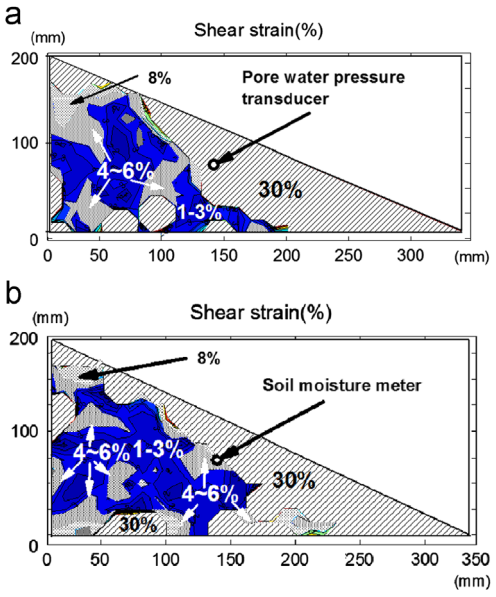

Fig. 9. Shear strain obtained from PIV analysis for Toyoura sand slope: (a) at peak degree of pore water pressure and (b) at peak degree of saturation.

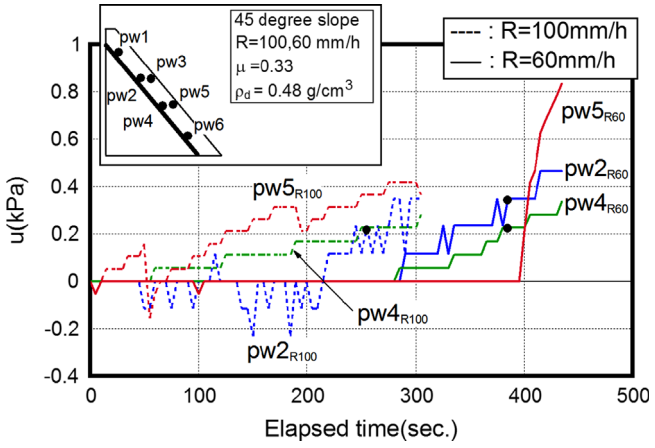

Fig. 11. Changes in pore water pressure with elapsed time for Kashiwabara volcanic slope.

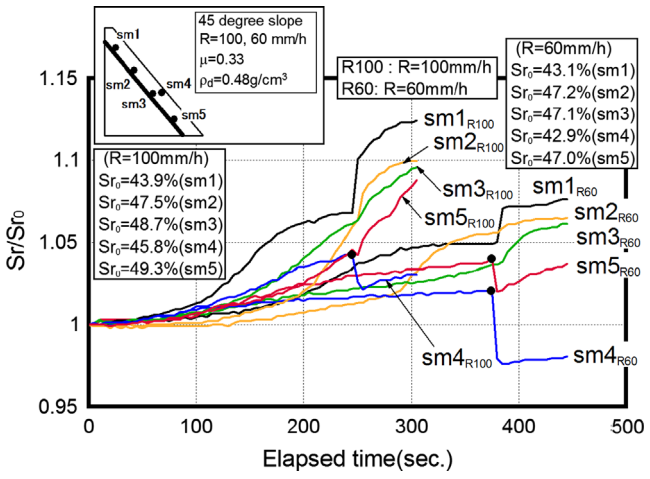

Fig. 10. Changes in saturation degree with elapsed time for Kashiwabara volcanic slope.

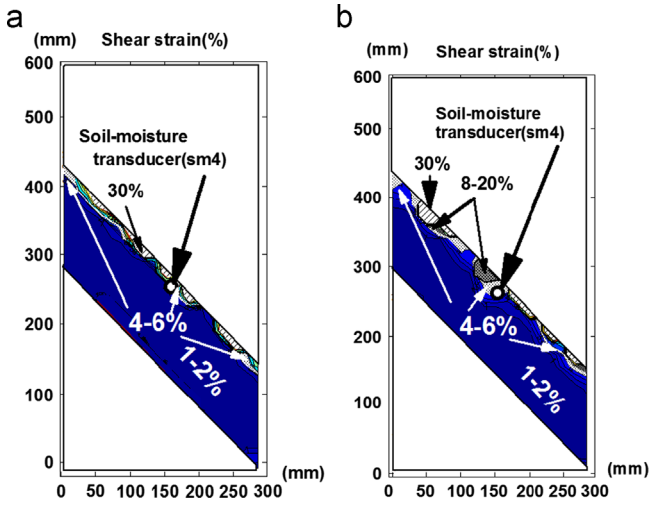

Fig. 12. Shear strain at peak degree of saturation obtained from PIV analysis for Kashiwabara volcanic slope: (a) $R=100$ mm/h and (b) $R=60$ mm/h.

Test results and discussions

Surface failure of volcanic slopes due to rainfall

Before commencing discussions on the failure patterns of volcanic slopes subjected to freeze–thaw action, the dependency of the slope angle and the initial water content on failure caused by rainfall was investigated for unsaturated volcanic slopes.

Fig. 13(a) and (b) shows typical deformation behavior at failure for 55- and 65-degree slopes for Touhoro volcanic soil (see cases 1 and 3). In the figures, the slip line observed in the model test is depicted as a dotted line. The initial water content of each slope, w_0, is 65%. It is obvious from these figures that the deformation behavior changes depending on the magnitude of the slope angle. For example, the depths of the collapse area for a 55-degree slope are deeper than those for a 65-degree slope. Such a dependency of the slope angle on the collapse area has been observed in the field (e.g., Scheidegger, 1973).

For the behavior of saturation normalized by initial value Sr_0, the ratio of the saturation degree for a 55-degree slope gradually increases compared with that for a 65-degree slope (see Fig. 14(a) and (b)). The saturation degree around the collapse area increased and then suddenly decreased with the increase in void ratio due to the large deformation. For example, the data of sm4 is significant. On the other hand, pore water pressure Δu is normalized by initial overburden pressure σ'_{vo}, and $\Delta u/\sigma'_{vo}$ around the slip line seems to develop just before failure (see Fig. 15(a) and (b)). A similar tendency was observed in the data for Kashiwabara volcanic soil (e.g., Kawamura et al., 2010a).

Photograph 1(a) and (b) illustrates the deformation behavior of the failed 45- and 65-degree slopes for the Komaoka

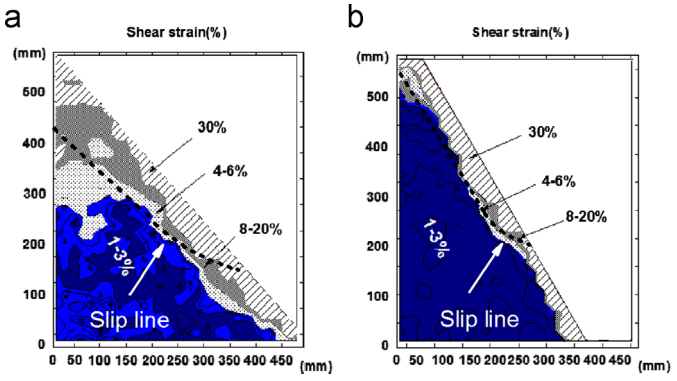

Fig. 13. Typical deformation behavior (shear strain) at failure for Touhoro volcanic slope: (a) 55 degree slope and (b) 65 degree slope.

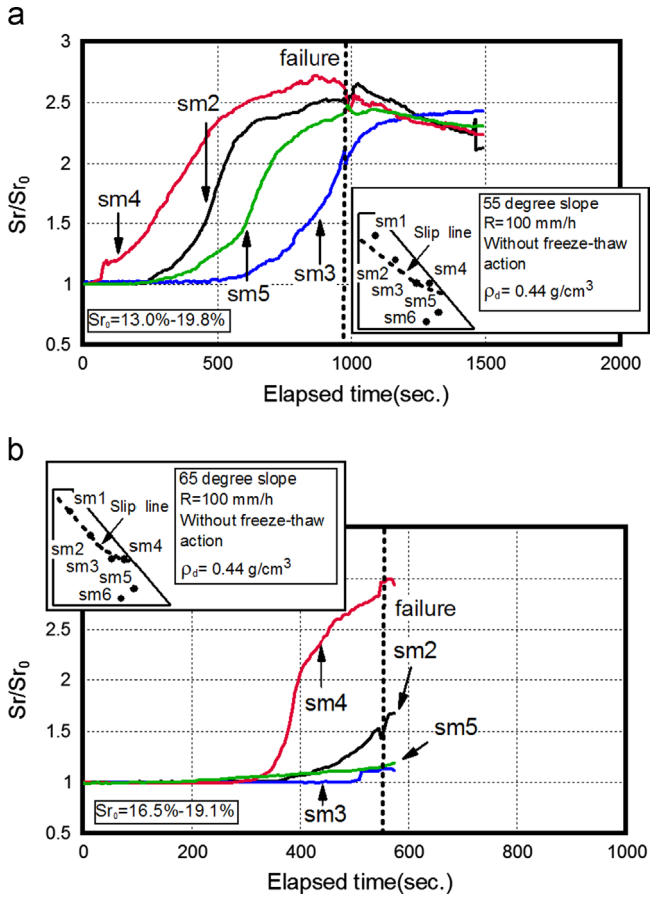

Fig. 14. Changes in saturation degree during rainfall test for Touhoro volcanic slope: (a) 55 degree slope and (b) 65 degree slope.

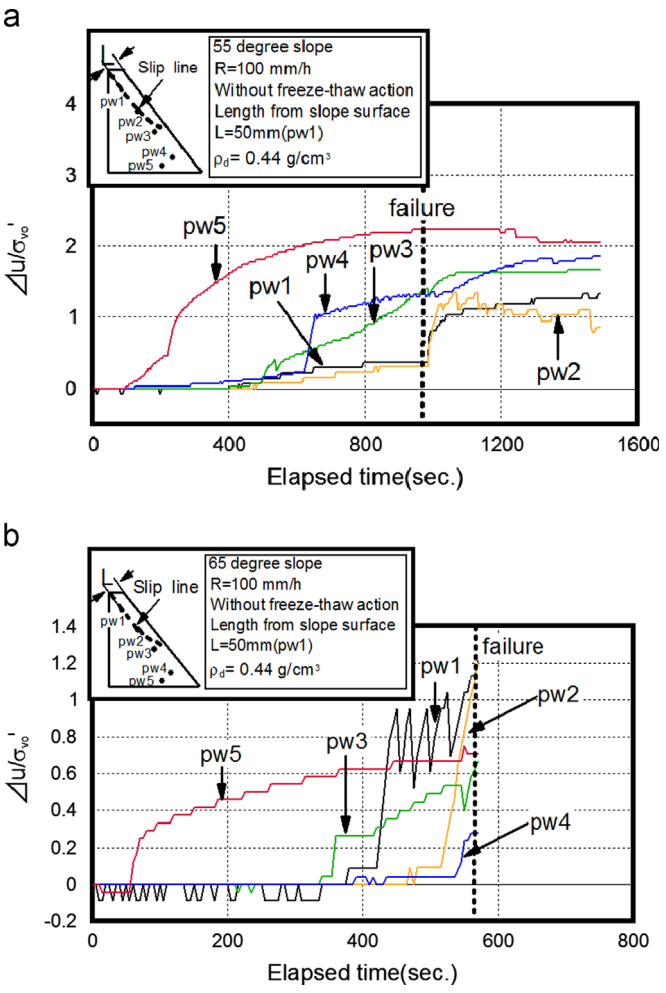

Fig. 15. Behavior of pore water pressure during model test for Touhoro volcanic slope: (a) 55 degree slope and (b) 65 degree slope.

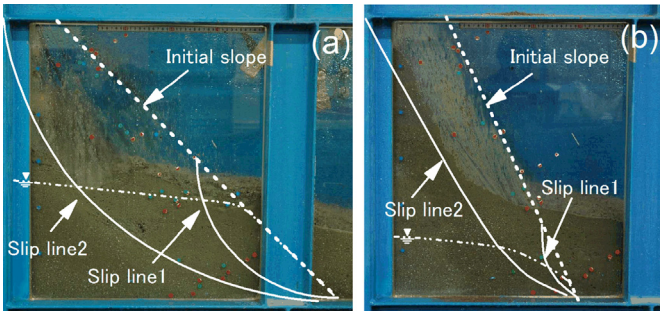

Photograph 1. Typical shape of failed slope for Komaoka volcanic soil: (a) 45 degree slope and (b) 65 degree slope.

volcanic soil (see cases 6 and 8). As shown in the photograph, the depths of the collapse area for the 45-degree slope are deeper than those for the 65-degree slope, similar to those of the other volcanic soils. However, the difference in failure patterns between Komaoka and Touhoro volcanic soils was recognized; the first failure (slip line 1) was generated at the toe of slopes, and the second failure (slip line 2) was induced with the increase in the groundwater level for each slope irrespective of the difference in slope angle. Regarding the behavior of the pore water pressure, the pressure ratios around slip line 1 increased gradually until $\Delta u/\sigma'_{vo}=1$ or more, thereafter the ratios around slip line 2 similarly increased again (see Fig. 16(a) and (b)). Although the difference in behavior seems to be dependent on the characteristics of the soil materials, the behavior of the pore water pressure explains the above failure phenomenon well. From the results, it is important to grasp the characteristics of the water retention capacity of the soil materials and how saturation and pore water pressure develop in the slopes.

Fig. 17 depicts the relationships between the slope angle and the elapsed time up to failure under the same initial water contents for three kinds of volcanic soil (see cases 1–3, cases 6–8, cases 11 and 12). For Kashiwabara volcanic soil, the test cases for two slope angles were plotted in the figure because slope failure was not induced when slope angles were less than 55 degrees and slopes could not be formed at more than 65 degrees. It is evident from the figure that the elapsed time preceding failure accelerates with an increase in slope angle. In general, it is well known that phenomena such as that observed above are attributed to the magnitude of the slope angle. In consideration of the model test results, therefore, it is pointed out that the difference in slope angle affects the characteristics of seepage, the collapse area and slope stability due to rainfall.

In order to clarify the effect of the difference in initial water content on the mechanical behavior of unsaturated volcanic slopes, Photographs 2 and 3 illustrate typical states of failed shapes for Kashiwabara and Touhoro volcanic soils, where the initial water contents are w_0=70 and 40% for the Kashiwabara volcanic soil (65-degree slope), and w_0=80 and 45% for the Touhoro volcanic soil (55-degree slope), respectively (see cases 12 and 1). As shown in these photographs, the shapes of the failed slopes are different for each volcanic slope. In particular, the slopes with lower water contents fail at shallower depths than those with higher water contents.

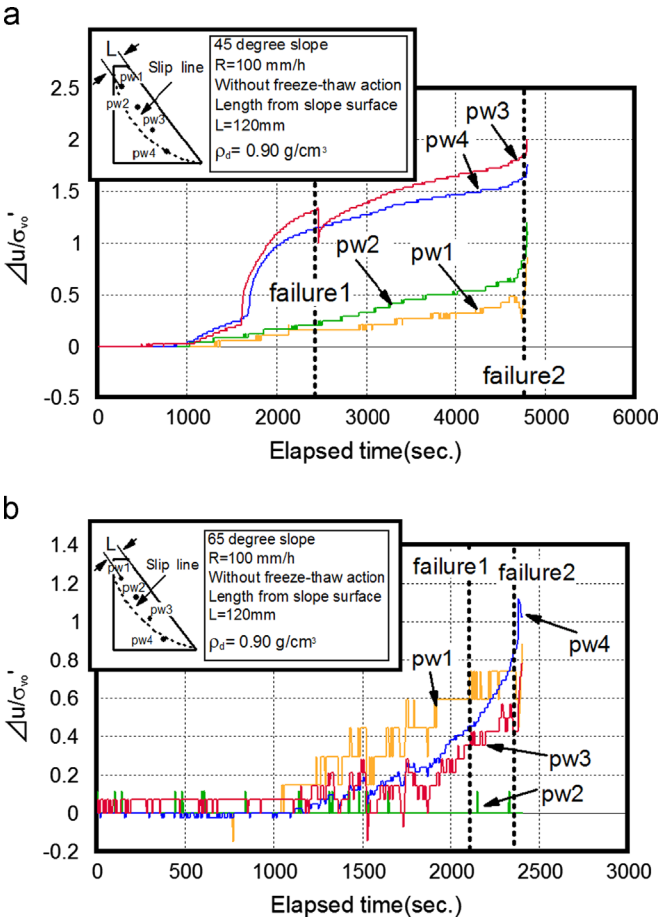

Fig. 16. Behavior of pore water pressure during model test for Komaoka volcanic slope: (a) 45 degree slope and (b) 65 degree slope.

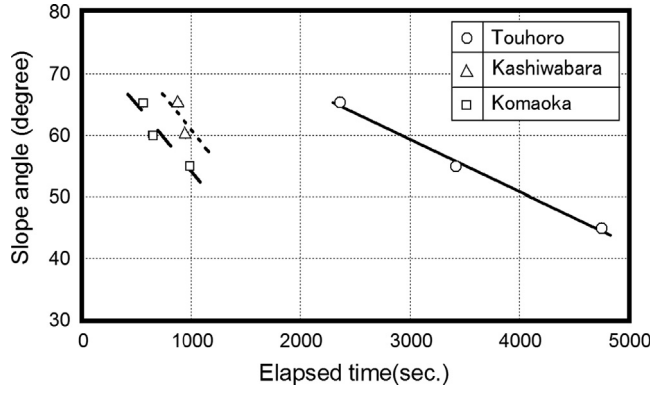

Fig. 17. Relationship between slope angle and elapsed time until failure.

Changes in the saturation degree for Touhoro and Kashiwabara volcanic slopes are shown in Fig. 18(a) and (b) (see cases 3 and 12). In these figures, the data of sm1, which is placed around the slip line, are typically depicted. As shown in the figure, the changes in elapsed time and in the magnitude of the saturation degree attributed to the difference in w_0 are recognized for each soil. For example, each value of elapsed time is 180 s for 20%, 760 s for 40% and 860 s for 70% in the Kashiwabara volcanic soil. In the case of lower water contents, seepage water due to rainfall can be retained in voids in the

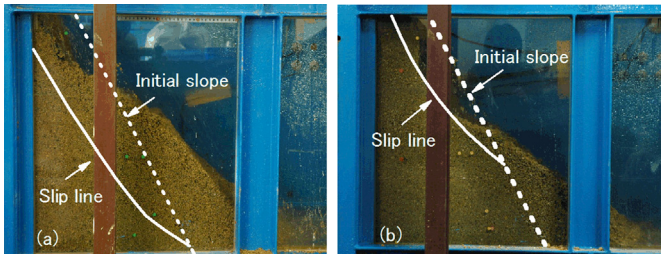

Photograph 2. Typical shape of failed slope for Kashiwabara volcanic soil: (a) $w_0=70\%$ and (b) $w_0=40\%$.

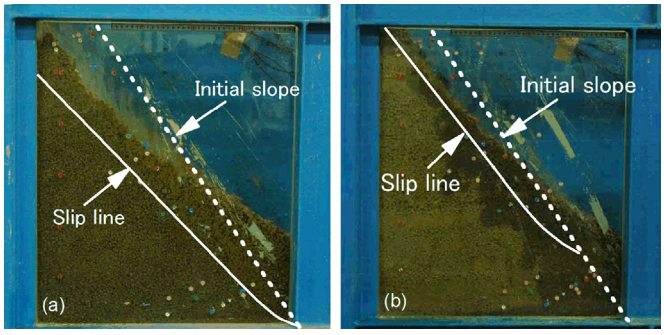

Photograph 3. Typical shape of failed slope for Touhoro volcanic soil: (a) $w_0=80\%$ and (b) $w_0=45\%$.

slope because its velocity becomes slower. As a result, surface slope failure is rapidly caused due to the increase in self-weight around the shallower areas of the Kashiwabara volcanic slopes (Kawamura et al., 2010a). Ishikawa et al. (2009) have revealed the unsaturated mechanical behavior of Kashiwabara volcanic soil using element test devices. According to their research, the permeability of volcanic soil decreased when the saturation degree was less than around 60%.

On the other hand, changes in elapsed time and in magnitude of the saturation degree for the Touhoro volcanic soil are different from those of the Kashiwabara volcanic soil (see Fig. 18(a)). The reason for this is that Touhoro volcanic soil has a high ability to retain water due to the soil particles being more porous and crushable compared to the Kashiwabara volcanic soil (Nakata and Miura, 2006). This indicates that the depth of the slip line and failure modes change depending on the increase in water retention capacity with seepage for such volcanic soils.

In comparison to typical behavior of pore water pressure in the case of $w_0=65\%$ for Touhoro volcanic soil (see Fig. 15 (b)), the pore water pressure around the slip line gradually increased until failure (see Fig. 19); however, its behavior is not sensitive compared to that of the degree of saturation. For this reason, it is important to monitor the changes in water content to predict slope failure.

As mentioned above, the difference in the development of the degree of saturation due to an increase in pore water pressure and seepage force is one of the causes of slope failure. More specifically, slope failure appears to be induced by the expansion of areas with high water retention. Presented herein

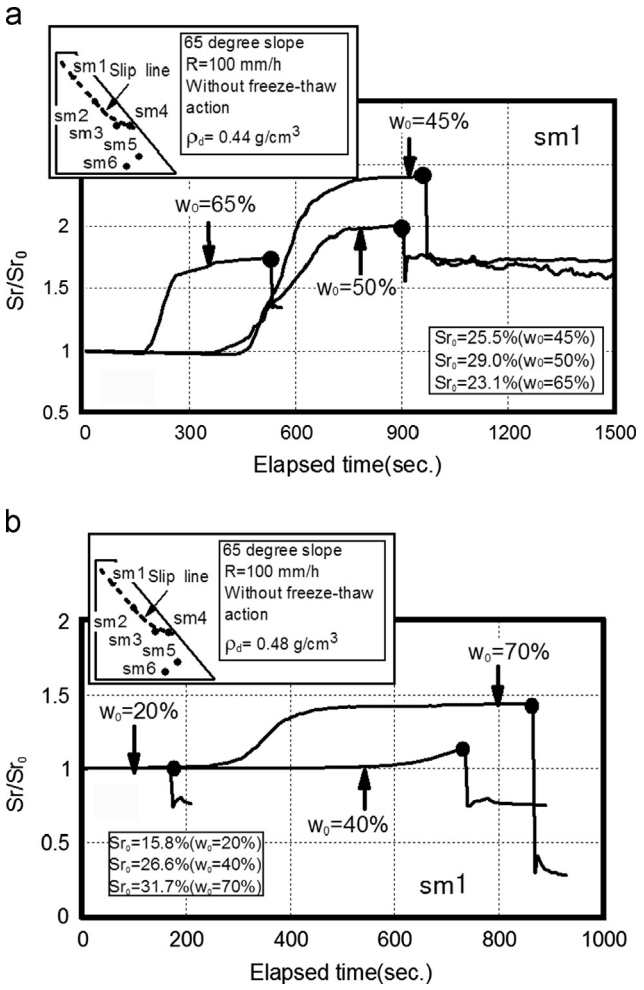

Fig. 18. Typical changes in saturation degree until failure: (a) Touhoro volcanic slope and (b) Kashiwabara volcanic slope.

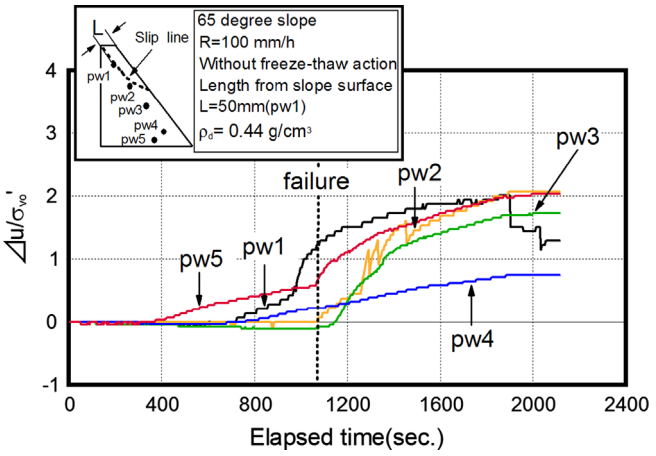

Fig. 19. Behavior of pore water pressure during test for Touhoro volcanic slope, $w_0=65\%$.

is a prediction method for slope failure of such volcanic slopes which takes into account water retention characteristics. Based on the results of all test data (see cases 1–3, cases 6–8, cases 11 and 12), the relationships between the initial water content, w_0, and the water content at failure, w_f, are shown in Fig. 20.

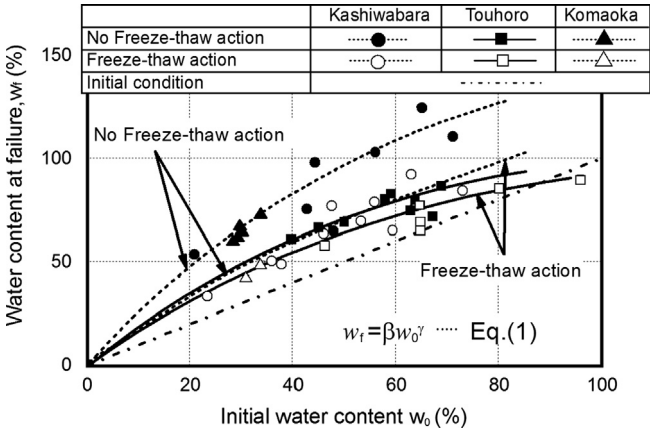

Fig. 20. Relationship between initial water content and water content at failure for each volcanic slope.

In this figure, the test data for freeze–thaw action, which will be described in a latter discussion, are additionally depicted (see cases 4 and 5, cases 9 and 10, cases 13–17). The water retention capacity was calculated as water content. From the figure, it is evident that there are unique relationships between both water contents. In particular, note that the ratio of the increase in water content becomes a constant with the increase in initial water content. For instance, the following expression can be obtained:

$$w_f = \beta \cdot w_0^{\gamma} \quad (1)$$

where β and γ are coefficients (these values are shown in Table 5). As shown in the table, it is interesting that there is no difference in γ among these volcanic soils and that the β of the Kashiwabara and Komaoka volcanic soils, which were sampled from the same volcano ejecta, demonstrated the same values. This may indicate that the features of seepage and water retention capacity depend on the ejecta of particular volcanos and can be evaluated uniquely. In any case, further consideration is required.

For example, slope stability will be evaluated according to the following procedure, based on Fig. 20 and Eq. (1).

(1) Estimate the line of water content w_f to cause slope failure, as mentioned above.
(2) Investigate the initial water content at the setting positions of measurement instruments, such as soil moisture meters.
(3) Monitor the change in water content due to the increase in rainfall or snowmelt.
(4) If the monitoring data on water content reaches the predicted line, shown by Eq. (1), the destabilization (failure) of the slope will be predicted.

In such way, it is possible to evaluate slope stability if such a relation can be obtained for an in situ slope, and slope failure can be predicted if the water retention capacity in a slope is estimated by monitoring the index properties, such as the water content.

Rainfall induced failures of volcanic slopes subjected to freezing and thawing

On the basis of the above test results, three types of rainfall model tests with freeze action or freeze–thaw action were carried out, namely one was a model test on model slopes with a frozen layer as an impermeable layer (see case 14), while the others were model tests on model slopes subjected to freeze–thaw action (see cases 4 and 5, cases 9 and 10, cases 15–17). For the model test on the frozen layer as an impermeable layer, an outer layer with a thickness of 100 mm was formed on a frozen layer (see Photograph 4) by pluviating the same volcanic soil under the same construction procedure conditions; therefore, the stress history was only freeze action. For the model tests on the model slopes subjected to the freeze–thaw action, the surface of the slope was frozen with dry ice over a period of 8 h, and then it was thawed at a temperature of 20 °C over a period of 8 h after the model slope was constructed; thereafter, a rainfall test was performed until failure. Typical changes in temperature ($T1$–$T9$) in the model slopes during the freeze–thaw action for each material are depicted in Fig. 21(a–c). As shown in these figures, temperatures decreased during the freezing action (until around 28,800 s). Thereafter, they increased with the lapse of time. In particular, the values at the depth of 25 mm ($T1$, $T4$ and $T7$) were approximately less than 0 °C, although the changes in temperature differed for each soil.

Table 5
Coefficients of β and γ.

Sample name and coefficients	Kashiwabara		Komaoka		Touhoro	
	β	γ	β	γ	β	γ
No freeze–thaw action	2.4	0.9	2.4	0.9	4.3	0.7
Freeze–thaw action	2.8	0.8	2.8	0.8	2.4	0.8

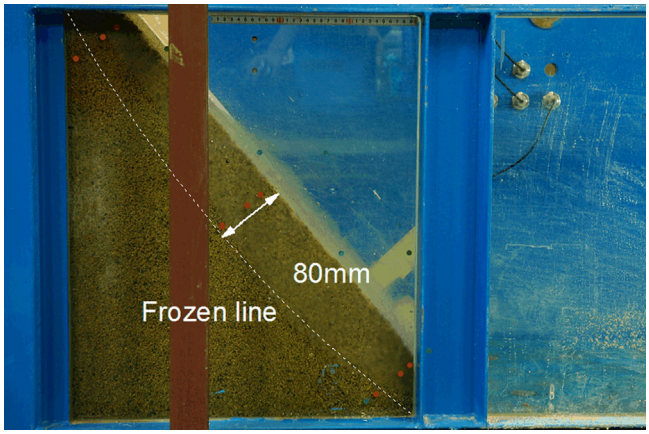

Photograph 4. Shape of model slope having frozen layer as impermeable layer for Kashiwabara volcanic soil.

Effect of frozen layer as impermeable layer (failure pattern 1)

Photograph 5 and Fig. 22 depict the slope shape and the deformation behavior of the Kashiwabara volcanic slope at the peak degree of saturation in the case of the freeze action (see case 14), compared with the case of an impermeable layer under the same surface friction as reported in previous studies (e.g., Kawamura et al., 2010a). The slope angle and the dry density are 65° and 0.45 g/cm^3, respectively. As can be seen in the photo and the figure, there appears to basically be no difference in deformation behavior at the peak degrees of saturation between the slopes with a frozen layer and with an impermeable layer. During rainfall testing, the saturation degree of sm4 gradually increases with an increase in rainfall; thereafter, it suddenly decreases (see Fig. 23). These failures were caused in the same deformation pattern. This fact denotes that the formation of a frozen layer in the spring season is a key factor for evaluating the stability of volcanic slopes, as shown in Fig. 1(b). This is similar to the case of the impermeable layer (Kawamura et al., 2010a). According to these results, it is anticipated that the degree of saturation in a frozen layer suddenly increases with thawing action from a condition of low to high saturation in the spring season. It can be pointed out that there is the possibility that the process of thaw action has an influence on the failure mechanisms.

Kawamura et al. (2010a) also revealed the effect of the thawing time (speed) on the failure mechanisms. As a result, it was shown that the effect of the thawing time on the mechanical behavior of model slopes changed depending on the variation in the initial water content for Kashiwabara

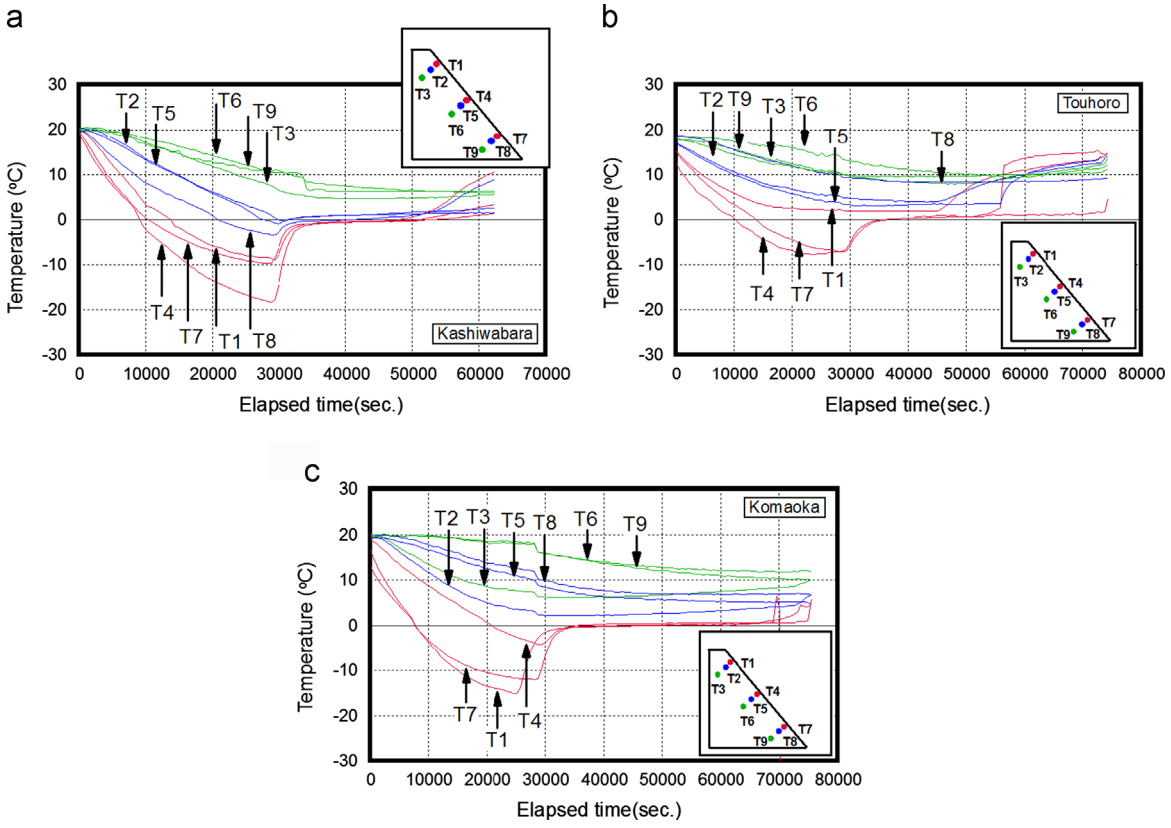

Fig. 21. Typical changes in temperature during freeze–thaw action: (a) Kashiwabara volcanic slope, (b) Touhoro volcanic slope, and (c) Komaoka volcanic slope.

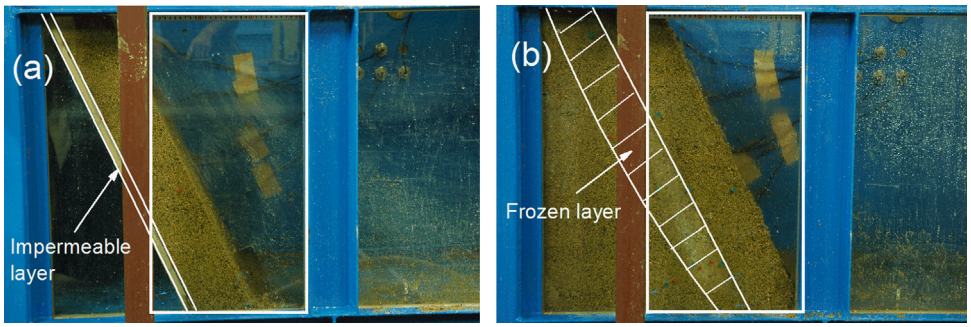

Photograph 5. Deformation state of Kashiwabara volcanic slope at peak degree of saturation: (a) impermeable layer and (b) frozen layer.

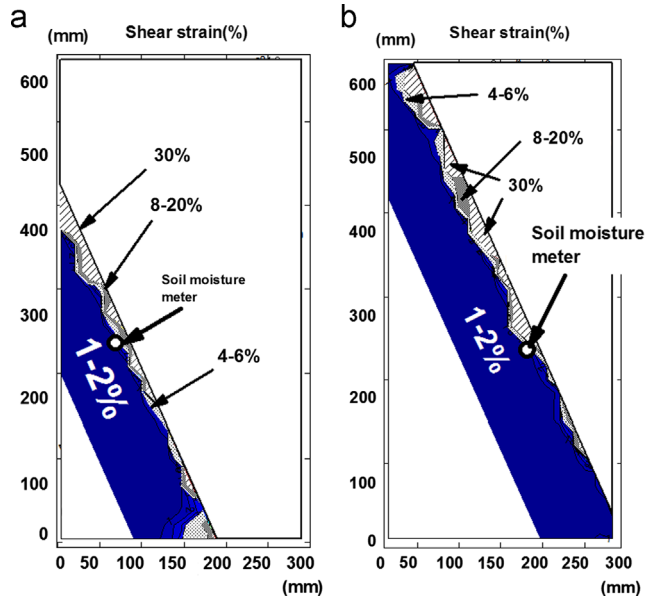

Fig. 22. Deformation behavior (shear strain) of Kashiwabara volcanic slope at peak of saturation degree (PIV analysis): (a) impermeable layer and (b) frozen layer.

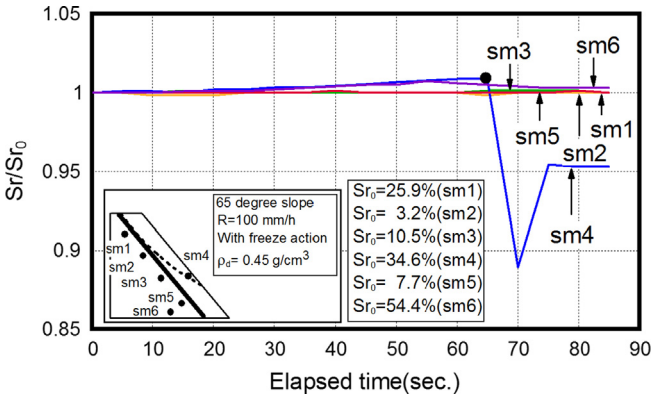

Fig. 23. Changes in saturation degree during rainfall test for Kashiwabara volcanic slope.

volcanic slopes. The effect may also have an influence on the variation in pore water pressure due to the increase in water from snowmelt. Due to this, changes in failure patterns can be predicted. Further consideration will be given to this matter in a subsequent discussion (failure pattern 2).

Effect of freeze–thaw action (failure pattern 3)

Based on the above results, model tests were performed on volcanic slopes subjected to freeze–thaw action. Fig. 24(a) and (b) shows the changes in the normalized degree of saturation during rainfall tests after freeze–thaw action for Kashiwabara volcanic soil, compared to the changes without freeze–thaw action (see cases 12 and 17). It can be seen that Sr_0 at sm6 indicates a high value. The reason for this is that sm6 was set to 15 mm from the bottom and its area became highly saturated due to the effect of seepage water. Each degree of saturation gradually increases, and then suddenly decreases after failure

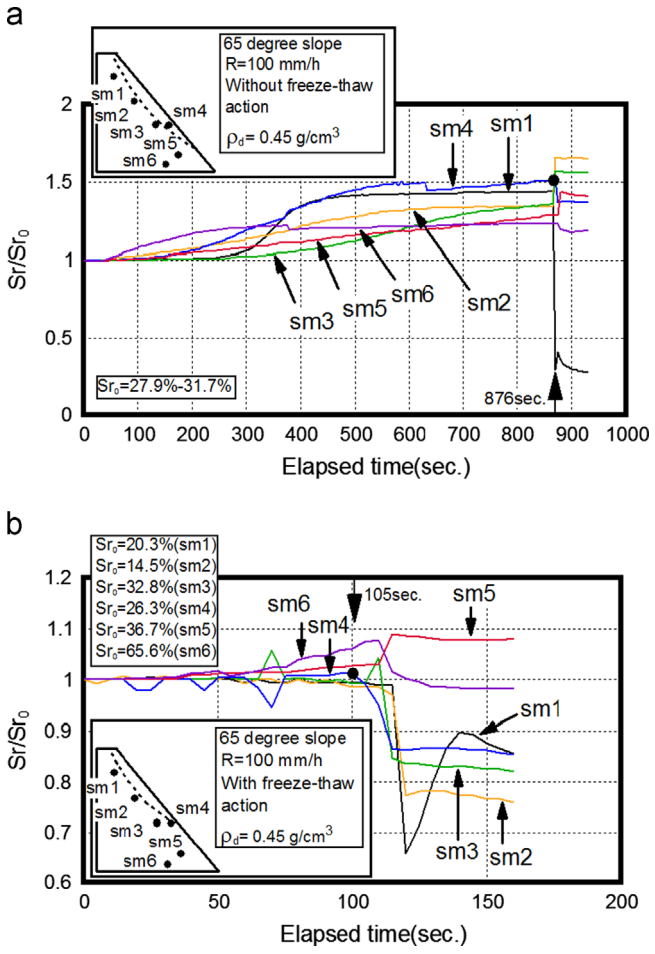

Fig. 24. Changes in saturation degree during rainfall test for Kashiwabara volcanic slope: (a) no freeze–thaw action and (b) freeze–thaw action.

(see the black symbol). It is also noted that there is a difference in elapsed time until failure between the two cases. For example, the elapsed time subjected to freeze–thaw action (105 s) is around nine times faster than that without (876 s).

Typical changes in the degree of saturation and pore water pressure for Touhoro and Komaoka volcanic soils are shown in Figs. 25 and 26 (see cases 5 and 9). In comparison to the no freeze–thaw action for Touhoro volcanic soil (see Figs. 14(b) and 15(b)), it was found that there is no difference in the development of saturation between the two volcanic soils, but that the difference in elapsed time until failure is apparently confirmed. For example, the elapsed time subjected to freeze–thaw action is 384 s, which is around 1.5 times faster than that without (557 s). A similar tendency was obtained from the data for Komaoka volcanic soil (see Fig. 26). Ishikawa et al. (2009) have also revealed the effect of freeze thaw action on the hydraulic behavior of Kashiwabara volcanic soil subjected to freeze thaw action using element test devices. For the results, it was clarified that the coefficient of permeability of freeze-thawed specimens decreased as compared with that of non freeze-thawed ones under the same degree of saturation. The reason seems to be because of the realignment of the constituent particles of the Kashiwabara volcanic soil caused

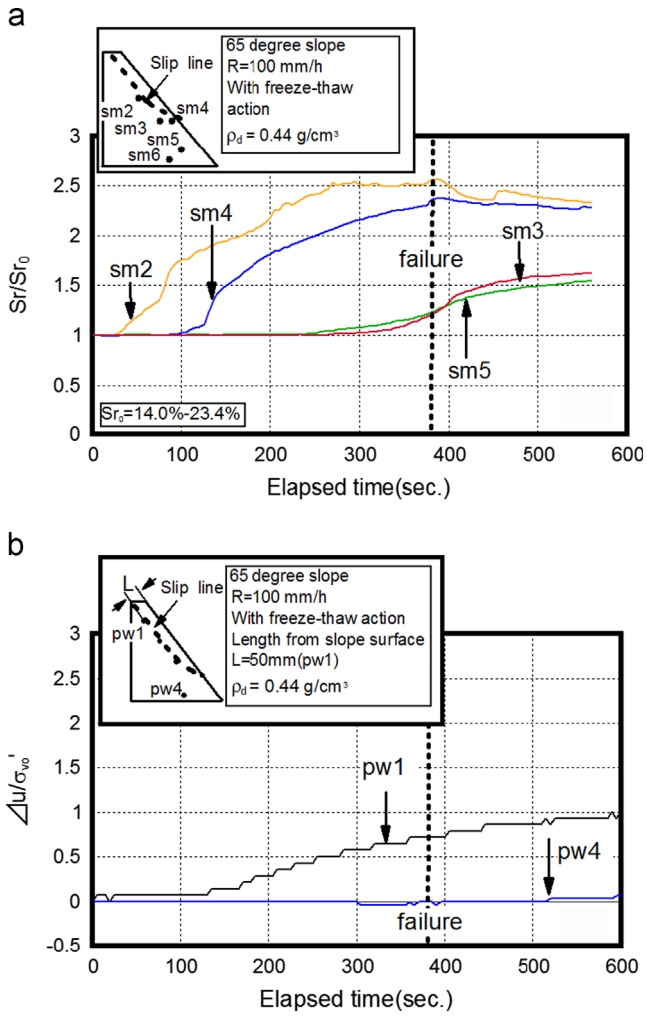

Fig. 25. Changes in saturation degree and pore water pressure for Touhoro volcanic slope: (a) saturation degree and (b) pore water pressure.

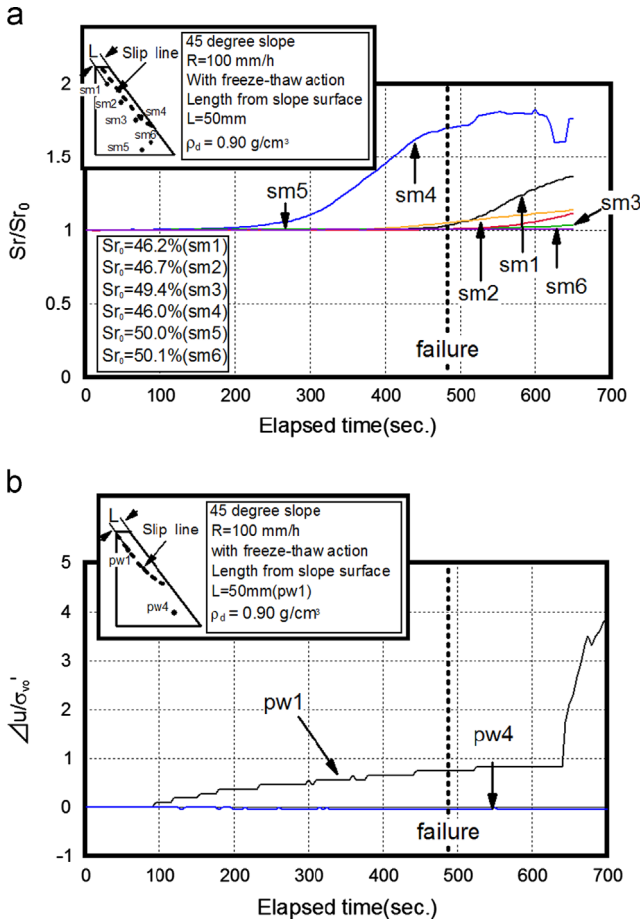

Fig. 26. Changes in saturation degree and pore water pressure for Komaoka volcanic slope: (a) saturation degree and (b) pore water pressure.

by freezing and thawing. Therefore, this fact seems to explain the above results well.

In order to clarify the influence of freeze thaw action on the deformation behavior of model slopes, Figs. 27–29 illustrate the deformation behavior (the distributions of shear strain) during freeze–thaw action for Kashiwabara, Touhoro and Komaoka volcanic soils, respectively. In Fig. 27, deformation vectors are also indicated for Kashiwabara volcanic soil. As the figures demonstrate, the shear strain increases with freezing and becomes a constant value during thawing for each volcanic slope. The typical deformation vectors are approximately perpendicular to the surface during freezing action, and change its direction due to gravity during thawing action. The variation in density can also be confirmed, as shown in the inserted photograph in Fig. 27. This fact indicates that hollows caused by thawing generate loose structures in the frozen layer compared with before the freeze–thaw process (as shown in Fig. 1(d)). A similar tendency was observed in the field monitoring data on a cut slope in Hokkaido, Japan (Kawamura and Miura, 2011)

In addition, the effect of the number of freeze–thaw cycles on the deformation behavior was investigated in this study. Yamaki et al. (2009) reported that the number of freeze–thaw cycles was six during the winter season (from December 8, 2007 to April 1, 2008) in the city of Sapporo in Hokkaido, Japan. They also indicated that the reduction ratio of the shear modulus of the volcanic ground, due to an increase in freeze–thaw cycles, reached a steady state at around two freeze–thaw action cycles. In this study, therefore, two freeze–thaw action cycles were adopted (see cases 4, 9 and 17).

For the test on the Kashiwabara volcanic slope subjected to two freeze–thaw action cycles (see Fig. 30), the change in vertical strain $\Delta\varepsilon v_i$ during the freeze action gradually decreases with an increase in freeze–thaw action, where i denotes the number of freeze–thaw cycles, $N_{F\text{-}T}$. The schematic diagram for changes in the vector in the slope during the freeze–thaw sequence is also depicted in Fig. 31. A similar tendency, in which vertical strain decreases with an increase in the freeze–thaw cycle, was indicated for Touhoro and Komaoka volcanic slopes and the results of element tests on volcanic soil (Yamaki et al., 2009), although images of these results are not provided. These facts imply that the deformation changes from a perpendicular to a gravitational direction during freezing and thawing, and that its effect is predominant in the first cycle of the model test.

Figs. 32–34 show typical changes in volumetric strain during the freeze–thaw sequence for Kashiwabara, Touhoro and Komaoka volcanic soils where contraction was expressed

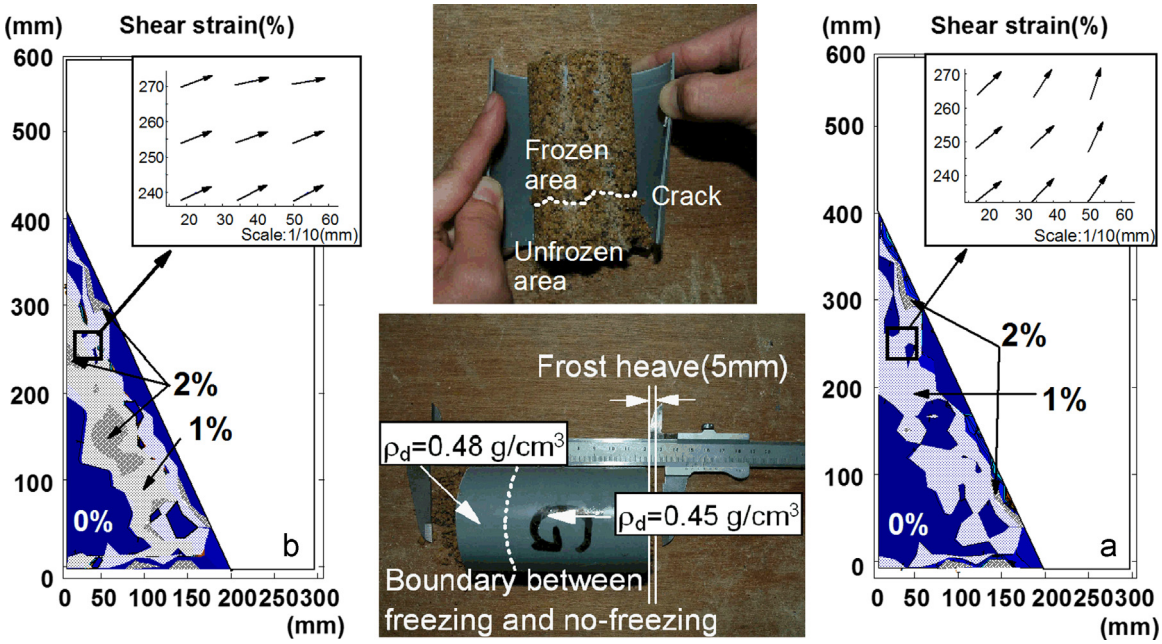

Fig. 27. Deformation behavior (shear strain) of Kashiwabara volcanic slope (PIV analysis): (a) after freeze action and (b) after thaw action.

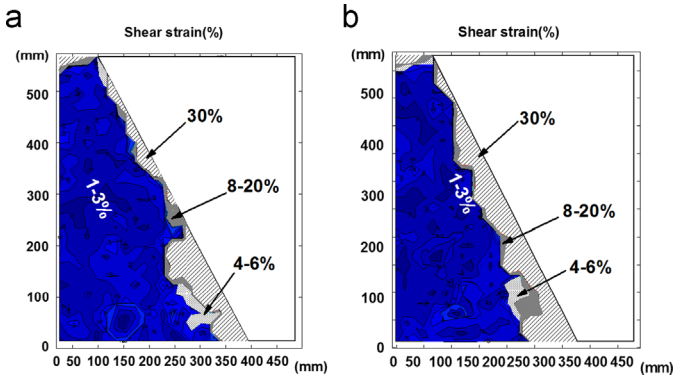

Fig. 28. Deformation behavior (shear strain) of Touhoro volcanic slope (PIV analysis): (a) after freeze action and (b) after thaw action.

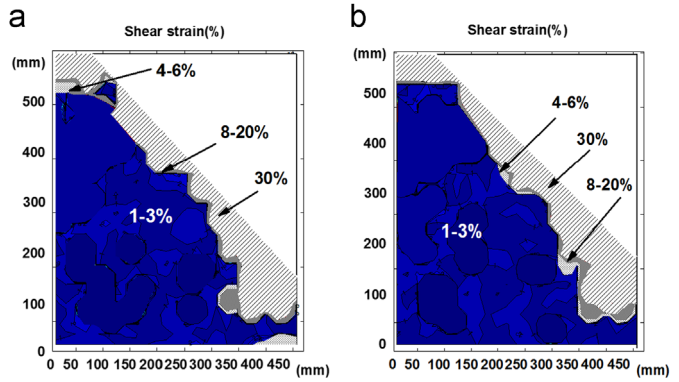

Fig. 29. Deformation behavior (shear strain) of Komaoka volcanic slope (PIV analysis): (a) after freeze action and (b) after thaw action.

as a minus (−) (see cases 4, 9 and 17). The initial water contents are w_0= 70%, 65% and 34% for Kashiwabara, Touhoro and Komaoka volcanic soils, respectively. In the

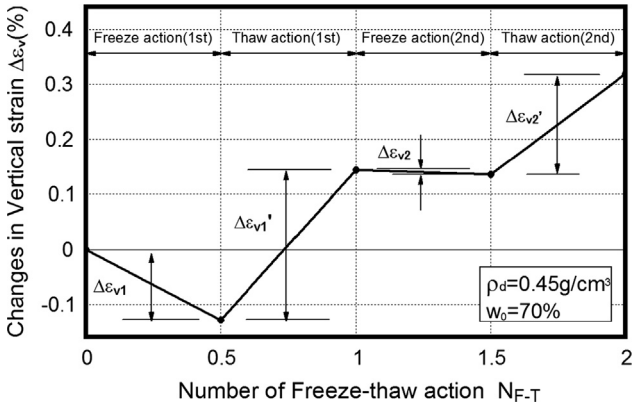

Fig. 30. Changes in vertical strain during freeze–thaw sequence for Kashiwabara volcanic slope.

figures, although the dilatancy around the surface indicates a contractive tendency (−) for the initial stage of the first cycle for the Kashiwabara volcanic slope (see Fig. 32(a)), it indicates an expanding tendency during freezing action for all the test materials (see Fig. 32(b), Fig. 33(b) and Fig. 34(b)). For the second cycle, the behavior is almost the same as that after the freezing action of the first cycle (see Figs. 32(d), 33(c) and 34(c)). To examine this behavior further, comparisons of the depths of slip line *Ds* and frozen layer D_f, observed in the model test, are shown in Fig. 35. This figure demonstrates that the depth is almost the same for each case. From the results, it can be said that such volcanic slopes subjected to freezing and thawing action have already been in the plastic equilibrium state. Therefore, if the change in dilatancy of a slope can be estimated, the influence of the freeze–thaw action on the surface slope failure can be evaluated accurately and its area of influence may be predicted if the depth of the frozen areas for in situ slopes can be estimated by field monitoring devices.

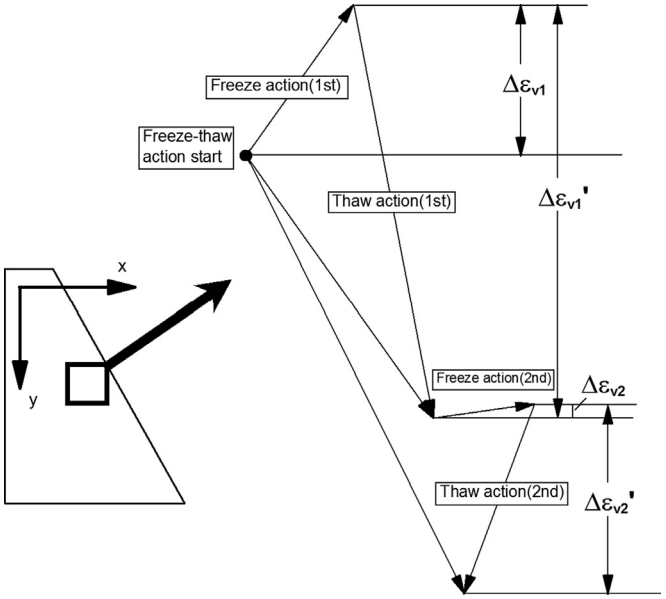

Fig. 31. Schematic of changes in vector in slope after freeze–thaw actions.

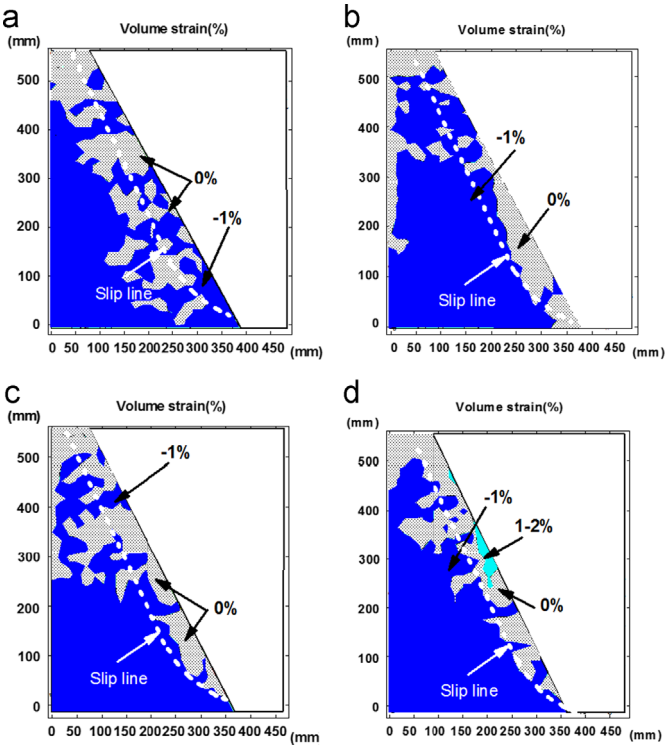

Fig. 32. Deformation behavior (volumetric strain) after freeze–thaw action for Kashiwabara volcanic slope: (a) freeze action (after 2 h), (b) after freeze action, (c) after thaw action, and (d) after thaw action at second.

As previously discussed, the influence on failure mechanisms was characterized by natural events such as rainfall, freezing and thawing. Similarly, the effects of the material characteristics of soils were investigated, for instance, the particle breakage of volcanic soils during model testing.

A comparison of the distribution of grain size after tests for the Touhoro volcanic slopes is shown in Fig. 36 (see cases 3 and 5). It is evident from the figure that the grain-size

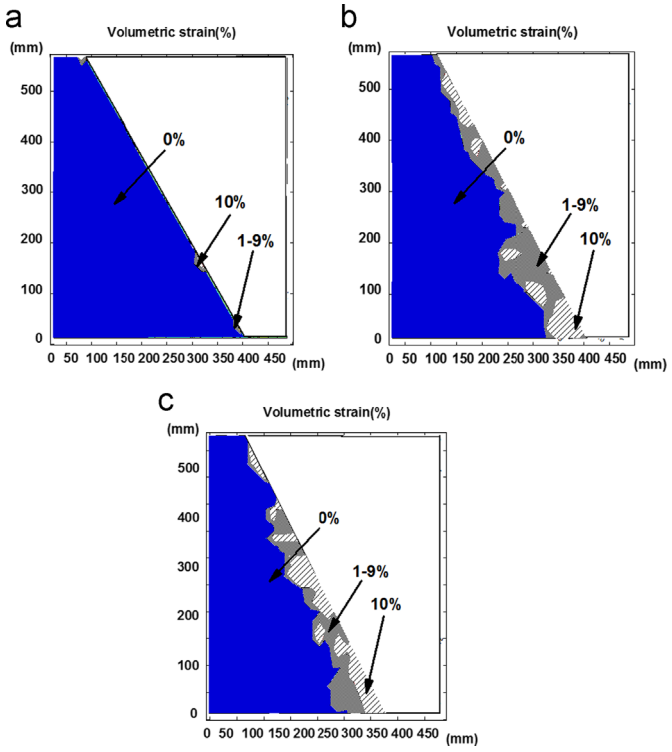

Fig. 33. Deformation behavior (volumetric strain) after freeze–thaw action for Touhoro volcanic slope: (a) freeze action (after 1 h), (b) after freeze action, and (c) after thaw action at second.

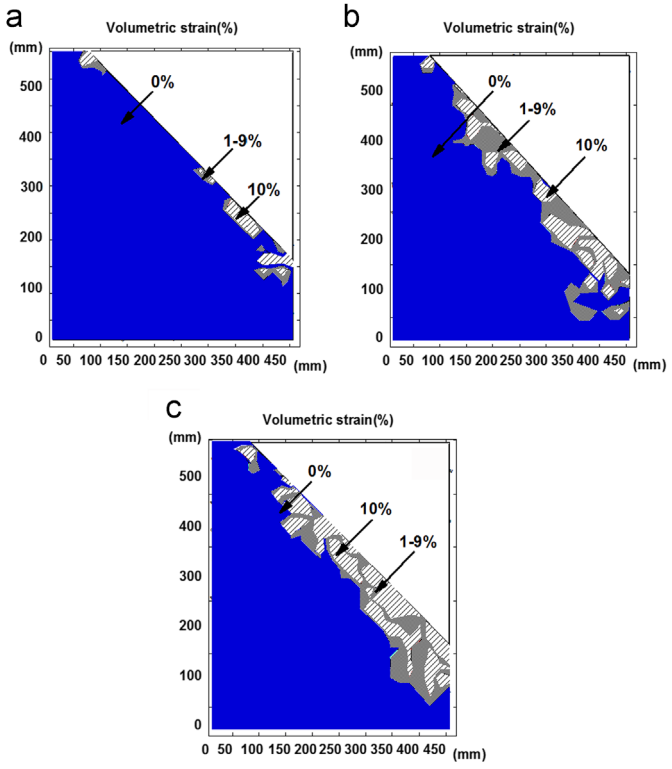

Fig. 34. Deformation behavior (volumetric strain) after freeze–thaw action for Komaoka volcanic slope: (a) freeze action (after 1 h), (b) after freeze action, and (c) after thaw action at second.

distribution varies by the freeze–thaw action, in particular, the case of w_0 =100% was significant among all test cases. Fig. 37 illustrates the increment in fines content before and after the tests, ΔFc (%), for each type of volcanic soil. ΔFc increases with the increase in the initial water content. It is interesting that particle breakage increases with stress histories, such as rainfall and freeze–thaw action. This implies that the failure of unsaturated volcanic slopes with crushable particles is derived not only by loose structures due to the freeze–thaw action, but also the reduction in shearing resistance due to particle breakage during rainfall and freeze–thaw action. The reduction in shearing resistance due to particle breakage was described by Miura et al. (1996) and Yagi and Miura (2004). An accurate estimation of the softening of slope surfaces by the freeze–thaw action is important for the stability of volcanic slopes; in particular, its influence is attributed to the reduction in the shearing resistance due to particle breakage.

Effect of existence of frozen layer (failure pattern 2)

The failure pattern shown in Fig. 1(c) was finally clarified. A series of model tests with an increase in groundwater was performed on the Kashiwabara volcanic slope after a thawing

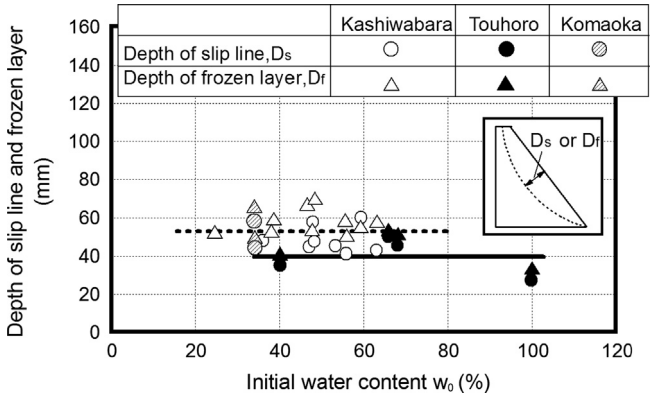

Fig. 35. Comparison of depths of slip line D_s with frozen layer D_f after rainfall test.

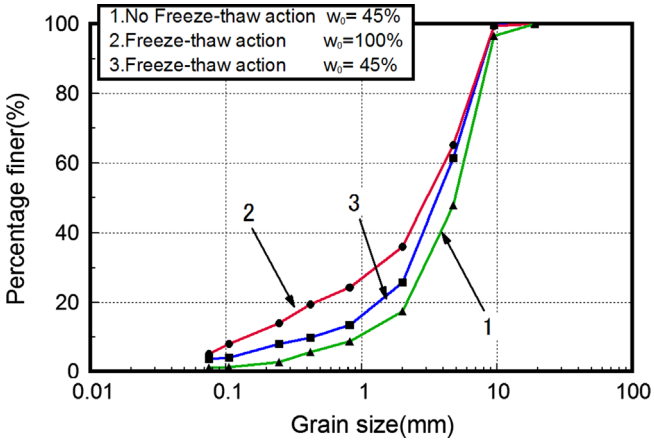

Fig. 36. Changes in grain size distribution after rainfall test for Touhoro volcanic slope.

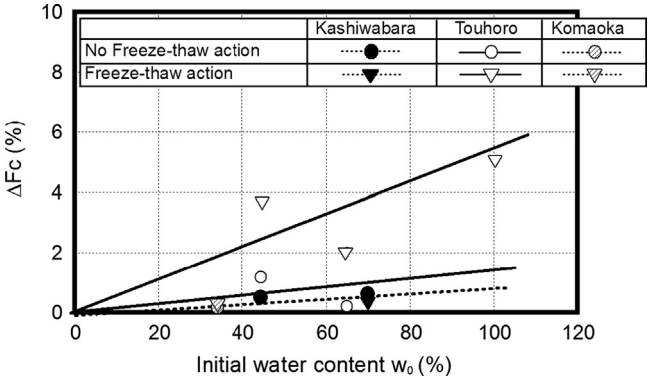

Fig. 37. Changes in increment of finer content ΔF_C after rainfall test.

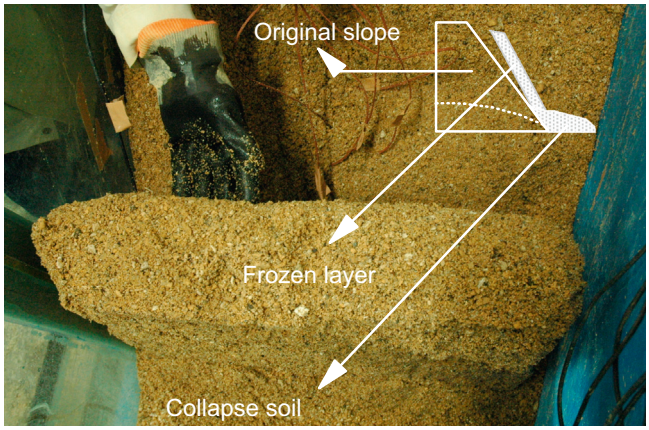

Photograph 6. Part of frozen layer separated from original slope after model test.

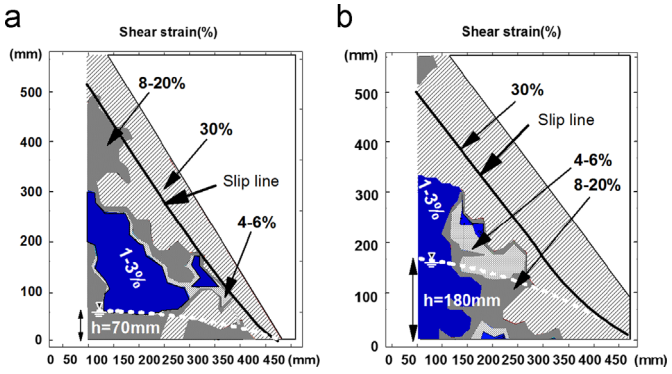

Fig. 38. Deformation behavior (shear strain) at failure for Kashiwabara volcanic slope: (a) no freeze–thaw action and (b) freeze–thaw action.

period of 1 h (see cases 13 and 15). Fig. 38(a) and (b) shows typical deformation behavior of the Kashiwabara volcanic slope for a 60-degree slope with and without freeze–thaw process. In the figures, a slip line observed in the model test is also depicted as a solid line. It is obvious that the groundwater level increases in the case of the freeze-thaw process, and then slope failure with a slip line is induced. The groundwater level changed from h=70 mm to h=180 mm; thereafter, slope failure was gradually induced in the toe area of the slopes. Furthermore, the collapse area was larger than that without the freeze–thaw action. Photograph 6 illustrates

the part of the frozen layer which was separated from the original slope after the model testing. In this way, a thick frozen layer can actually be observed in the volcanic slope. This means that a deeper slope failure is induced by an increase in pore water pressure due to the existence of a frozen layer in the snowmelt season. Therefore, the existence of a frozen layer is significant for cold regions not only in terms of the action of the impermeable layer, but also as the cause of an increase in the groundwater level due to snowmelt water or rainfall during the spring months.

Fig. 20 also shows the relationship between the water content at failure and the initial water content for all data for the freeze–thaw action cases (failure patterns 1, 2 and 3). It is clearly seen that there are unique relationships between the two water contents and those of the non-freeze–thaw action, although the water content at failure decreases. This indicates that void structures of constituent particles are loose structures due to freezing and thawing. It can also be said that slope failure can be predicted if the water retention capacity in a slope is estimated for volcanic slopes subjected to freeze–thaw action, as shown in Eq. (1).

Considering the results of the model tests, failure patterns in cold regions were clarified and their evaluation methods were investigated. However, the above results may change with variations in soil materials and inherent errors, such as the scale effect. In any case, further investigations in this direction are required.

Conclusions

On the basis of the limited amount of model testing conducted in this study, the following conclusions were derived:

(1) Changes in surface slope failure depend strongly on the slope angle and the initial water content.
(2) The softening of slopes by freeze–thaw action is important for evaluating the stability of volcanic slopes. In particular, its effect is attributed to the reduction in shearing resistance due to particle breakage and cannot be ignored in evaluations of slope stability.
(3) A slope subjected to freezing and thawing deforms perpendicularly and in an upward direction on its surface for freezing. Its direction changes to a gravitational course for thawing, and has already been in the plastic equilibrium state. If the change in dilatancy of a slope is estimated, the influence of the freeze–thaw action on surface slope failure can be evaluated.
(4) Slope failure can be predicted if the depth of the frozen area and the water retention capacity in the slope are estimated by monitoring index properties, such as water content.

Acknowledgments

The authors wish to express their sincere gratitude to Messrs. Y. Sato, M. Ashihara, K. Okuda, H. Ino, H. Nakano and D. Shimazu, who conducted a major part of the experiments (Muroran Institute of Technology, Japan), and to Dr. T. Ishikawa and Dr. S. Yokohama (Hokkaido University). This study was undertaken with the financial support of KAKENHI (Grant-in-Aid for Science Research (B) No. 16310121, (A) No. 19201035 and (A) No. 23241056), Japan Society for the Promotion of Science.

References

Aoyama, O., Ogawa, S., Fukuda, M., 1985. Temperature dependencies of mechanical properties of soils subjected to freezing and thawing. In: Proceedings of the Fourth International Symposium on Ground Freezing, 217–222.

Harries, C., Davies, M.C.R., 2000. Gelifluction: observations from large-scale laboratory simulations. Arctic, Antarctic and Alpine Research 32 (2), 202–207.

Harries, C., Lewkowicz, A.G., 2000. An analysis of the stability of thawing slopes, Ellesmere island, Nunavut, Canada. Canadian Geotechnical Journal 37, 449–462.

Ishikawa, T., Ozaki, Y., Miura, S., 2008. Influence of freeze–thaw action on mechanical behavior of crushable volcanic coarse-grained soils. Journal of Geotechnical Engineering, JSCE III-64 (3), 712–717 in Japanese.

Ishikawa, T., Miura, S., Tokoro, T., 2009. Effect evaluation of freeze–thaw action on hydro-mechanical behavior of unsaturated granular materials In: Proceedings of the 17th International Conference on Soil Mechanics and Geotechnical Engineering, ISSMGE, vol. 1, 833–836.

Ishikawa, T., Miura, S., Ito, K., 2010. Influence of freeze–thaw action on mechanical behavior of unsaturated crushable volcanic soil. In: Proceedings of the Fifth International Conference on Unsaturated Soils, 549–554.

Jeng, C.-J., Lin, T.-A., 2011. A case study on the in-situ matrix suction monitoring and undisturbed–sample laboratory test for the unsaturated colluvium slope. Soils and Foundations 51 (2), 321–331.

JGS, Hokkaido Branch, 2010. A Guideline on Countermeasures on Frost-Heaving Damage of Slopes, The Research Committee in Hokkaido Branch, JGS, 1–125 (in Japanese).

JGS, Hokkaido Branch, 2011. Volcanic Soils for Engineers—Characteristics, Design, Construction and Disasters. The Research Committee in Hokkaido Branch, JGS, 1–130 (in Japanese).

JSCE, 2004. Reconnaissance Report of the Typhoon 10th, 2003, ⟨http://ws3-er.eng.hokudai.ac.jp/flood2003/index.htm⟩, The Reconnaissance Committee of the Typhoon 10th (in Japanese).

JSSMFE, 1995. Reconnaissance Report of the 1993 Kushiro-oki Earthquake and Notohanto-oki Earthquake, The Reconnaissance Committee of 1993 Kushiro-oki and Notohanto-oki Earthquake (in Japanese).

Kasama, K., Jiang, Y., Hiro-oka, A., Yasufuku, N., Sato, H., 2011. Geo- and hydro-mechanical evaluation of slope failure induced by torrential rains in Northern-Kyusyu area, July 2009. Soils and Foundations 51 (4), 575–589.

Kawamura, S., Kohata, K., Ino, H., 2007. Rainfall-induced slope failure of volcanic coarse-grained soil in Hokkaido. In: Proceedings of the 13th Asian Regional Conference on Soil Mechanics and Geotechnical Engineering, ISSMGE, 931–934.

Kawamura, S., Miura, S., Ishikawa, T., Yokohama, S., 2010a. Rainfall-induced failure of unsaturated volcanic slope subjected to freeze–thaw action and its evaluation. Journal of Geotechnical Engineering, JSCE C-66 (3), 577–594 in Japanese.

Kawamura, S., Miura, S., Yokohama, S., 2010b. Mechanical behavior of anisotropic sand ground beneath structures subjected to cyclic loading such as wave loading. Soils and Foundations 50 (5), 645–657.

Kawamura, S., Miura, S., 2011. Stability evaluation of slope subjected to rainfall and freeze–thaw actions based on field monitoring. Advances in Civil Engineering (Online Access Journal), 2011, 14 pages, Hindawi Publishing Corporation.

Kitamura, R., Sako, K., Kato, S., Mizushima, T., Imanishi, H., 2007. Soil tank test on seepage and failure behaviors of Shirasu slope during rainfall. Japanese Geotechnical Journal, JGS 2 (3), 149–168 in Japanese.

Kitamura, R., Sako, K., 2010. Contribution of "Soils and Foundations" to studies on rainfall-induced slope failure. Soils and Foundations 50 (6), 955–964.

Kojima, H., Obayashi, S., Kitamura, R., 2003. An application of satellite thermal infrared data in trigger-factor inverse estimation for identifying hazardous-slope composed of Shirasu-deposit. Journal of Geotechnical Engineering, JSCE III-61 (749), 99–110 in Japanese.

Miura, S., Yagi, K, Kawamura, S., 1996. Static and cyclic shear behavior and particle crushing of volcanic coarse grained soils in Hokkaido. Journal of Geotechnical Engineering, JSCE III-36 (547), 159–170 in Japanese.

Miura, S., Yagi, K., Asonuma, T., 2003. Deformation-strength evaluation of crushable volcanic soils by laboratory and in-situ testing. Soils and Foundations 43 (4), 47–57.

Nakata, T., Miura, S., 2006. Changes in void structures due to particle breakage of volcanic coarse-grained soil. Journal of Geotechnical Engineering, JSCE C-63 (1), 236–243 (in Japanese).

Nishimura, T., Ogawa, S., Wada, T., 1993. Influence of freezing and thawing on suction and shearing strength of unsaturated soils. Journal of Geotechnical Engineering, JSCE III-24 (475), 59–67 in Japanese.

Okimura, T., 2006. The present situation and some problems for disaster prevention research and management of debris hazards caused by a heavy rainfall (theme: challenges to rainstorm-triggered disasters), Tsuchi-to-kiso, JGS, 55 (6), 1–4 (in Japanese).

Olivares, L., Damiano, E., Greco, R., Zeni, L., Picarelli, L., Minardo, A., Guida, A., Bernini, R., 2009. An instrumented flume to investigate the mechanics of rainfall-induced landslides in unsaturated granular soils. Geotechnical Testing Journal, ASTM 32 (2), 108–118.

Orense, R., Farooq, K., Towhata, I., 2004. Deformation behavior of sandy slopes during rainwater infiltration. Soils and Foundation 44 (2), 15–30.

Scheidegger, A.E., 1973. On the prediction of the reach and velocity of catastrophic landslides. Rock Mechanics 5, 231–236.

Torii, N., Okimura, T., Kato, S, 2007. Experimental study on slope failure mechanism induced by rainfall after earthquake. Journal of Geotechnical Engineering, JSCE C-63 (1), 140–149 in Japanese.

White, D.G., Take, W.A., Bolton, M.D., 2003. Soil deformation measurement using particle image velocimetry (PIV) and photogrammetry. Geotechnique, (53), 619–631.

Yagi, N., Yatabe, R., Enoki, M., 1990. Prediction of slope failure based on amount of rain fall. Journal of Geotechnical Engineering, JSCE III-13 (418), 65–73 in Japanese.

Yagi, K., Miura, S., 2004. Evaluation of mechanical characteristics for crushable volcanic soil ground. Journal of Geotechnical Engineering, JSCE III-66 (757), 221–234 in Japanese.

Yamazaki, T., Tomojiri, S., Sasaki, T., 2000. Highway Technology, vol. 16. Research Institute, Japan Highway Public Corporation, 75–81 (in Japanese).

Yamaki, M., Miura, S., Yokohama, S., 2009. Effect of freeze–thaw sequence on deformation properties of crushable volcanic soil. Journal of Geotechnical Engineering, JSCE C-65 (1), 321–333 in Japanese.

Yatabe, R., Yagi, N., Enoki, M., 1986. Consideration on prediction method for occurring time of slope failure during seepage of rainfall. Journal of Geotechnical Engineering, JSCE III-6 (376), 297–305 in Japanese.

Zhang, G., Qian, J., Wang, R., Zhang, J.-M., 2011. Centrifuge model test study of rainfall-induced deformation of cohesive soil slopes. Soils and Foundations 51 (2), 297–305.